Original Article

American Society for Neurochemistry

ASN Neuro
September-October 2017: 1–34

DOI: 10.1177/1759091417726607
journals.sagepub.com/home/asn

SAGE

Mitogen- and Stress-Activated Protein Kinase 1 Regulates Status Epilepticus-Evoked Cell Death in the Hippocampus

Yun-Sik Choi[1], Paul Horning[2], Sydney Aten[2], Kate Karelina[2], Diego Alzate-Correa[3], J. Simon C. Arthur[4], Kari R. Hoyt[3], and Karl Obrietan[2]

Abstract

Mitogen-activated protein kinase (MAPK) signaling has been implicated in a wide range of neuronal processes, including development, plasticity, and viability. One of the principal downstream targets of both the extracellular signal-regulated kinase/MAPK pathway and the p38 MAPK pathway is *M*itogen- and *S*tress-activated protein *K*inase 1 (MSK1). Here, we sought to understand the role that MSK1 plays in neuroprotection against excitotoxic stimulation in the hippocampus. To this end, we utilized immunohistochemical labeling, a *MSK1* null mouse line, cell viability assays, and array-based profiling approaches. Initially, we show that MSK1 is broadly expressed within the major neuronal cell layers of the hippocampus and that status epilepticus drives acute induction of MSK1 activation. In response to the status epilepticus paradigm, *MSK1* KO mice exhibited a striking increase in vulnerability to pilocarpine-evoked cell death within the CA1 and CA3 cell layers. Further, cultured *MSK1* null neurons exhibited a heighted level of N-methyl-D-aspartate-evoked excitotoxicity relative to wild-type neurons, as assessed using the lactate dehydrogenase assay. Given these findings, we examined the hippocampal transcriptional profile of *MSK1* null mice. Affymetrix array profiling revealed that MSK1 deletion led to the significant (>1.25-fold) downregulation of 130 genes and an upregulation of 145 genes. Notably, functional analysis indicated that a subset of these genes contribute to neuroprotective signaling networks. Together, these data provide important new insights into the mechanism by which the MAPK/MSK1 signaling cassette confers neuroprotection against excitotoxic insults. Approaches designed to upregulate or mimic the functional effects of MSK1 may prove beneficial against an array of degenerative processes resulting from excitotoxic insults.

Keywords

cell death, excitotoxicity, hippocampus, MAPK, MSK1, neuroprotection

Received March 28, 2017; Accepted for publication June 22, 2017

Introduction

The molecular signaling events that regulate neuroprotection and excitotoxic cell death have been an area of intensive investigation for many years. Beyond the well-established roles of a subset of signaling pathways that underlie either neuroprotection (e.g., the Nrf2-Antioxidant Response Element signaling pathway) or cell death (e.g., the intrinsic apoptotic pathway), numerous cell signaling events and gene networks have the capacity to confer both protection *and* to enhance vulnerability to potentially excitotoxic insults (Mattson, 2003; Calabrese et al., 2005; Culmsee and Landshamer, 2006; Rueda et al., 2016). Consistent with this idea, the extracellular signal-regulated kinase (ERK)/MAPK pathway

[1]Department of Pharmaceutical Science and Technology, Catholic University of Daegu, Gyeongbuk, Republic of Korea
[2]Department of Neuroscience, Ohio State University, Columbus, OH, USA
[3]Division of Pharmacology, Ohio State University, Columbus, OH, USA
[4]College of Life Sciences, University of Dundee, Dundee DD1 5EH, Scotland, UK

Corresponding Authors:
Karl Obrietan, Department of Neuroscience, Ohio State University, Graves Hall, Rm 4118, 333 W 10th Ave, Columbus, OH 43210, USA.
Email: obrietan.1@osu.edu
Kari R. Hoyt, Division of Pharmacology, Ohio State University, Riffe Building, Rm 412 496 W. 12 th Ave. Columbus, OH 43210, USA.
Email: hoyt.31@osu.edu
Yun-Sik Choi, Department of Pharmaceutical Science and Technology, College of BioMedical Science, Catholic University of Daegu Gyeongbuk, 712-702, South Korea.
Email: tiana@cu.ac.kr

has been shown to function as both a regulator of neuroprotective and cell death signaling pathways (reviewed in Hetman and Xia, 2000; Zhuang and Schnellmann, 2006; Cagnol and Chambard, 2010; Martin and Pognonec, 2010; Subramaniam and Unsicker, 2010). Along these lines, a large number of *in vitro* and *in vivo* studies have shown that the abrogation of ERK/MAPK signaling suppresses neuronal death induced by multiple apoptotic- and necrotic-mediated mechanisms (Alessandrini et al., 1999; Kuroki et al., 2001; Lesuisse and Martin, 2002; Pedersen et al., 2002; Park et al., 2004). In contrast with these findings, studies have also shown that the ERK/MAPK pathway facilitates neuronal cell survival (reviewed in Ballif and Blenis, 2001; Portt et al., 2011). For example, ERK/MAPK signaling has been shown to stimulate preconditioning-mediated neuroprotection (Gonzalez-Zulueta et al., 2000; Bickler et al., 2005) and to drive the expression of neuroprotective genes, including BCL-2 and *BDNF* (Hetman et al., 1999; Cheng et al., 2013).

These profoundly discordant observations regarding ERK/MAPK signaling and cell viability may be explained by the route of injury, duration of activation, and the subcellular localization of ERK (Hetman and Xia, 2000; Zhuang and Schnellmann, 2006; Cagnol and Chambard, 2010; Martin and Pognonec, 2010). Here, we chose to further our understanding of the role of MAPK signaling in neuroprotection by focusing on one of its principal effector kinases: *M*itogen- and *S*tress-activated protein *K*inase 1 (MSK1). MSK1 (and its homolog MSK2) is a serine/threonine kinase that is formed by two distinct functional domains: an autoregulatory C-terminal kinase and an N-terminal substrate kinase (reviewed in Hauge and Frodin, 2006; Arthur, 2008; Reyskens and Arthur, 2016). In addition to its regulation by the ERK/MAPK cascade, MSK1 is downstream of the p38/MAPK pathway (Deak et al., 1998; McCoy et al., 2005).

MSK1 is localized to the cell nucleus and functions as a regulator of chromatin structure and transcription factor activation. For example, MSK1 phosphorylates histone H3 and the transcription factors ATF-1 and CREB (Wiggin et al., 2002; Soloaga et al., 2003; and reviewed in Arthur, 2008; Vermeulen et al., 2009; Reyskens and Arthur, 2016). Notably, via its phosphorylation of CREB at Ser133 (and the resulting increase in CRE-mediated gene expression), MSK1 appears to be a key route by which the ERK/MAPK pathway triggers long-term forms of neuronal plasticity. Consistent with this idea, *MSK1*-deficient mice exhibit an array of synaptic and cognitive deficits (Chwang et al., 2007; Karelina et al., 2012; Correa et al., 2012). Further, MSK1 regulates progenitor cell proliferation in the subgranular zone of the dentate gyrus (Karelina et al., 2015), which could also contribute to the cognitive deficits observed in *MSK1* null mice.

As with signaling via the ERK/MAPK pathway (an upstream effector of MSK1), there are divergent findings regarding the role of MSK in cell death signaling, with reports showing that MSK is both protective and can enhance vulnerability to stress stimuli (Hughes et al., 2003; Kannan-Thulasiraman et al., 2006; Lang et al., 2015). Here, we furthered this line of inquiry and provide data showing that the MSK1 pathway plays an important role in conferring resistance against seizure-evoked cell death.

Materials and Methods

Mice

$MSK1^{-/-}$ mice (also referred to here as *MSK1* null mice) and $MSK1^{+/+}$ (also referred to here as MSK1 WT mice) were provided by Dr. J. Simon C. Arthur (University of Dundee, Dundee, Scotland) and bred at the Ohio State University. $MSK1^{-/-}$ and MSK1 WT mice were genotyped via PCR profiling of DNA isolated from tail biopsies: The PCR cycling conditions and primers are described by Wiggin et al. (2002). The $MSK1^{-/-}$ deletion line was bred into a C57Bl/6 line for >10 generations. For the experiments shown in Figures 2(d) and 3 to 7, which constitute the cell death profiling and array assays, experimental mice were derived from $MSK1^{+/-}$ breeder cages; hence, $MSK1^{+/+}$ (WT) and $MSK1^{-/-}$ littermates with the same genetic background were used. Standard C57Bl/6 mice, originally acquired from Jackson Labs, were used for the MSK1, pMSK1, and pERK1/2 expression profiling assays (Figures 1 and 2(a), (b), (c), (e), and (f)). For all studies, adult, 6- to 14-week-old mice were used. Animals were entrained to a standard 12:12 light/dark cycle and were allowed *ad libitum* access to water and food. The studies reported here were conducted in compliance with the Ohio State University Institutional Animal Care and Use Committee guidelines.

Pilocarpine-Induced SE

The pilocarpine model was used to induce status epilepticus (SE) (Curia et al., 2008). Initially, mice received an *i*ntra*p*eritoneal (IP) injection of atropine methyl nitrate (1.3 mg/kg in saline, Sigma, St Louis, MO). Thirty minutes later, mice were IP injected with pilocarpine (310 mg/kg, Sigma) diluted in physiological saline to evoke SE. The Racine grading scale (Racine, 1972) was used to assess seizure magnitude and SE onset. SE was defined as multiple Stage 5 motor seizures (tonic-clonic seizures observed in all four limbs, which resulted in a loss of balance) that persisted for ≥3 h. SE was not terminated with diazepam.

Immunohistochemistry

For all histological analysis, mice were sedated using ketamine/xylazine anesthetic (ketamine: 120 mg/kg of

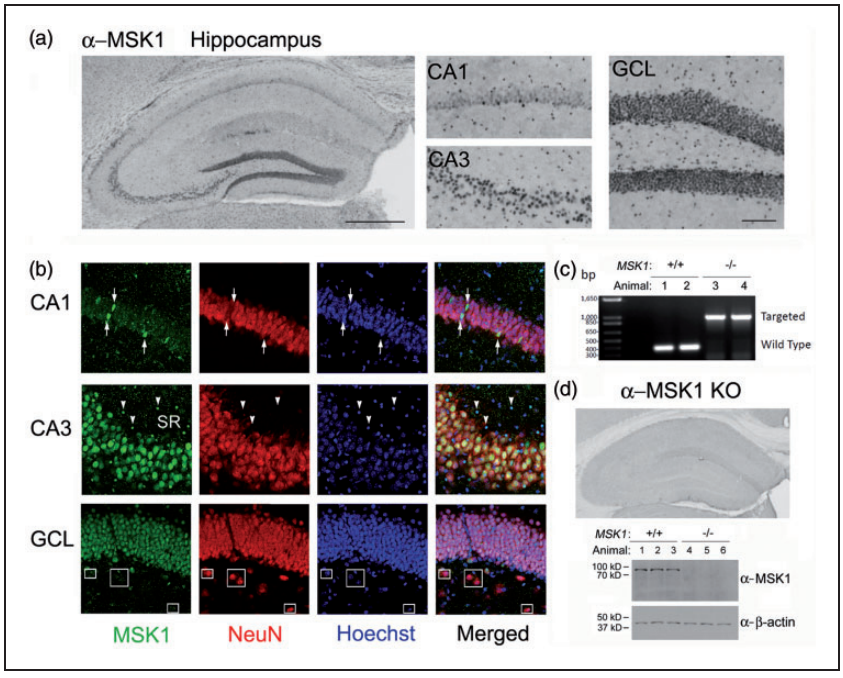

Figure 1. MSK1 expression in the hippocampus. (a) Immunohistochemical labeling revealed MSK1 expression within the principal hippocampal cell layers (CA1, CA3, and GCL). Bar: 400 μm (low magnification image). Bar: 50 μm (high magnification image). (b) Immunofluorescent double labeling for MSK1 and NeuN; colocalized expression was observed in the CA1, CA3, and GCL. CA1 panel: Arrows denote a subset of cells with high MSK1 expression. CA3 panel: Arrowheads denote nonneuronal cells with high MSK1 expression. SR: stratum radiatum. GCL panel: Boxes denote hilar interneurons with limited MSK1 expression. (c) PCR-based genotyping of the targeted (−/−) and WT (+/+) *MSK1* allele; tail biopsies were processed from two animals from each genotype. (d) Immunohistochemical labeling (top panel) and Western blotting (bottom panel) were used to confirm the loss of MSK1 protein in *MSK1* null mice.

body weight and xylazine: 24 mg/kg body weight), and tissue was fixed using transcardial perfusion with paraformaldehyde (4%) diluted in phosphate-buffered saline (PBS). Isolated whole brains were then postfixed in paraformaldehyde (4% for 4 h at 4°C) followed by cryoprotection using 30% sucrose. Stereotaxic coordinates from anterior to posterior from bregma: −1.40 to −2.20 mm were used to cut 40-μm coronal sections through the dorsal hippocampus.

Immunolabeling commenced with a series of wash steps in PBS, followed by incubation in PBS with 0.3% hydrogen peroxide. Next, the tissue was blocked (2 h at room temperature) using 10% normal goat serum or 3% normal horse serum diluted in PBS with 1% Triton X-100 (PBST). Sections were then immunolabeled (overnight at 4°C) using rabbit polyclonal anti-pMSK1 (1:1,000 dilution, Cell Signaling, Danvers, MA; catalog number: 9594) or rabbit polyclonal anti-pERK1/2 (1:1,000 dilution, Cell Signaling, catalog number: 9101). Next, the tissue was processed using the ABC labeling method and then incubated with horseradish peroxidase (HRP) avidin (Vector Labs; San Carlos, CA). Visualization of the immunolabeling was achieved by incubating the tissue with nickel-intensified diaminobenzidine substrate (Vector Labs) for HRP. Tissue was then mounted on gelatin-subbed slides, cleared with xylenes and coverslipped using Permount (Fisher Scientific). Photomicrographs were acquired using a Leica DM IRB microscope (Nussloch, Germany).

Cresyl Violet Staining

Mice were transcardially perfused, as described earlier, and 40-μm-thick sections through the hippocampus were mounted on gelatin-coated slides, dehydrated in alcohol, and stained in cresyl violet solution (0.3%). Next, the sections were destained (0.1% glacial acetic acid in 95% ethanol), cleared with xylenes, and finally coverslipped with Permount. Photomicrographs were acquired as described earlier.

Fluoro-Jade B

Fluoro-Jade B (FJB) labeling was performed using the methods described in Choi et al. (2007). Image collection was performed using a Zeiss 510 confocal microscope.

Cell Quantitation

Photomicrographs of cresyl violet and FJB-labeled cells were acquired at 40× magnification, and digital images were captured and data quantified using MetaMorph software (Universal Imaging, West Chester, PA). Quantitation

was performed on the CA1, CA3, and hilar regions of the hippocampus. The hilus was defined as the region between the lower and upper granule cell layer (GCL) blades. The total number of FJB- and cresyl violet-positive cells in each of four dorsal hippocampal sections were counted. Each section was separated by a 200-μm interval (stereotaxic coordinate AP, approximately −1.40 to −2.20 mm). Cell counts were averaged for each animal and then used to generate group mean ± SEM values for each condition. For the 3-day post-SE data sets, six to eight mice were used for each group; for the 6-week time points, four to six animals were used for each group. Data are reported as the mean ± the SEM for each condition. Mean values were statistically analyzed between cell layers (e.g., control vs. experimental) using the Student's t test, and a $p < .05$ was considered significant.

Immunofluorescent Labeling

Sections were washed with PBS and then blocked (2 h room temperature) with 10% normal goat serum in PBST. Next, sections were incubated overnight (at 4°C) with a rabbit polyclonal total MSK1 antibody (1:500 dilution, Cell Signaling, catalog number: 3489) and with a mouse monoclonal anti-NeuN antibody (1:1,000 dilution, Millipore, Billerica, MA; catalog code: MAB377). Tissue was then washed 5× in PBST and incubated for 2 h (at 22°C) with goat polyclonal Alexa 488- and donkey polyclonal Alexa 594- (1:1,000 dilution, Invitrogen, Carlsbad, CA) conjugated secondary antibodies. Next, sections were washed, and DNA was labeled with Hoechst (1 μg/ml: Cell Signaling). Finally, tissue was mounted with Cytoseal (Richard-Allan Scientific, Kalamazoo, MI), and images were acquired with a Leica SP8 confocal microscope.

Western Blotting

Animals were sacrificed as described earlier, and hippocampi were dissected from whole brains. Tissue was lysed in radioimmunoprecipitation assay buffer, and then protein extracts (5 μg/μL) were loaded onto 10% SDS-PAGE gels and electrophoresed and then transblotted onto polyvinylidene difluoride membranes (Immobilon-P; Millipore) using standard methodologies. Next, membranes were blocked with 10% milk in tris-buffered saline containing 0.1% Triton-X-100 (TBST: 1 hr) and then incubated overnight with the noted MSK1 (1:500 dilution) or pMSK (1:1,000, dilution) antibodies. After washing, membranes were treated (1 hr at room temperature) with an anti-rabbit IgG HRP-conjugated antibody (1:2,000 dilution, PerkinElmer Life Sciences), and the HRP signal was detected using the Renaissance bioluminescent detection system (New England Nuclear). Blots were then stripped and probed using a mouse monoclonal β-actin antibody (1:1,000, PhosphoSolutions Catalog code: 125-ACT), and the signal was detected using the noted HRP labeling and visualization steps.

RNA isolation and microarray analyses

Mice were sacrificed, and brains were isolated as described earlier. Bilateral hippocampal tissue was removed, and total RNA was purified using TRIzol (Invitrogen) following the manufacturer's protocol. RNA quantity and quality was assayed using an Agilent 2100 Bioanalyzer (Agilent Technologies), and the RNA from three animals per genotype (WT and *MSK1* null) was prepared for array profiling using the GeneChip one-cycle target labeling kit (Affymetrix). Biotinylated cRNA was profiled using the GeneChip 430 2.0 Mouse Genome Array, running one array per mouse: (e.g., three animals/arrays per genotype). cRNA preparation, microarray hybridization, and profiling were performed at the Ohio State University Microarray Core Facility. Raw data (.cel files) were processed using dChip software (http://www.hsph.harvard.edu/cli/complab/dchip/). The resulting data sets were filtered to identify genes that were significantly altered by the deletion of MSK1; a 1.25-fold change in expression with a p value of $\leq .05$ was considered significant. Subsequently, Matlab R2016a (MathWorks) was used to generate the hierarchical clustering map based on the expression values of significantly altered genes. Finally, gene functional classification and clustering were performed using the Database for Annotation, Visualization and Integrated Discovery (DAVID), with significant enriched annotation terms set to p values of $\leq .05$. Graphical representation of the analysis results was completed using the Cytoscape software Enrichment Map plug-in. Microarray data are available from the Gene Expression Omnibus website (http://www.ncbi.nlm.nih.gov/geo), under accession number: GSE98751.

Neuronal Toxicity Assays

Neuronal cell death after an N-methyl-D-aspartate (NMDA) challenge in primary hippocampal neurons from *MSK1* null and WT mice was assessed as described in Carrier et al. (2006). Briefly, neurons were isolated from the hippocampus of postnatal day 1 mice, dissociated with trypsin, and plated on polylysine-coated 12-mm glass coverslips in a 24-well plate. The cells were maintained in Neurobasal media supplemented with 2% B27, 1% penicillin/streptomycin, and 0.25 mM glutamine (all culture media were from Gibco) for 10 days. NMDA (50 μM) with 2 μM glycine (or control solution) was added to the cultures for 20 min, and the cell culture media was collected at 4 h and 8 h for the measurement of lactate dehydrogenase (LDH) release as a measure of loss of membrane integrity (measured as described in Carrier et al., 2006). Brightfield images of the cells were

also acquired as a record of cell health/death. Finally, at 8 h after NMDA/glycine treatment, cultures were fixed with 4% paraformaldehyde for 30 min at room temperature, permeabilized with 0.4% Triton X-100 for 10 min at 37°C, and blocked with 10% bovine serum albumin for 60 min at 37°C. The cultures were then incubated overnight (at 4°C) in monoclonal MAP2 antibody (1:500 dilution, HM-2 clone, Sigma, St. Louis, MO) in PBS containing 3% bovine serum albumin/0.4% Triton X-100. After washing (3×) with PBS, the cells were incubated 60 min (at 37°C) with an Alexa 488-conjugated antibody against mouse IgG (1:1000, Molecular Probes, Eugene, OR). Finally, the cells were stained with Hoechst (as described above), mounted on glass slides with PBS/glycerol (1:3), and sealed with nail polish. Fluorescence images were captured using a CoolSnap HQ digital camera (Roper Scientific, Tucson, AZ) connected to a Nikon TE2000S epifluorescence microscope (Nikon Instruments, Melville, NY). FITC excitation/emission filters were used to visualize MAP2 while DAPI filters were used for Hoechst 33258. Data were analyzed using MetaMorph software. Mean values were statistically analyzed between control and experimental conditions and between cell phenotypes using the Student's t test, and a $p < .05$ was considered significant.

Intracellular Calcium Measurement

Hippocampal neurons cultured on 12 mm coverslips were loaded with 5 μM Fura-2 AM (Molecular Probes) for 45 min at room temperature in a HEPES-based buffer (HBSS) containing the following (in mM): 137 NaCl, 5.6 glucose, 20 HEPES, 5 KCl, 0.6 Na_2HPO_4, 0.6 KH_2PO_4, 10 $NaHCO_3$, 0.9 $MgSO_4$, and 1.4 $CaCl_2$, pH 7.4. Coverslips were then placed in a laminar flow chamber and mounted on the stage of a Nikon TE2000S epifluorescence microscope. Single-cell ratiometric (alternating 340 nm/380 nm excitation wavelengths and 510 nm emission wavelength) fluorescence traces were acquired at 10-s intervals using MetaFluor software controlling a CoolSnap digital camera. Neurons were identified by morphology as assessed from bright-field images. Results are presented as background subtracted 340 nm/380 nm ratios. All NMDA-containing solutions were made in HBSS and contained 0.5 μM tetrodotoxin. NMDA solutions included 1 μM glycine and omitted $MgSO_4$. Mean-evoked response values were statistically analyzed between cell phenotypes using the Student's t test, and a $p < .05$ was considered significant.

Electroencephalogram Recording

Electroencephalogram (EEG) electrode placement, recordings, and analysis were performed as described in our previous study (Lee et al., 2009). Briefly, animals were surgically implanted with bipolar recording electrodes (Plastics One, Roanoke, VA): one within hippocampal area CA1 (anterior −1.8 mm from bregma; lateral 1.1 mm; and dorsoventral 1.2 mm) and the other within the cortex (anterior −2.8 mm from bregma; lateral 1.1 mm; and dorsoventral 1.2 mm). Animals were then allowed to recover from the electrode implantation procedure for 10 days prior to the initiation of the SE paradigm (described earlier). EEG recording was started 10 min prior to pilocarpine injection, and data were recorded for approximately 120 min post-SE onset. The MP150 data acquisition system (Biopac Systems, Santa Barbara, CA) was used to record polysomnographic signals, and data analysis was performed using Acknowledge 3.9.0 software (Biopac Systems). EEG data were analyzed at 10-min intervals, and the average peak-to-peak values were generated from 20-s EEG traces. Four WT and 4 *MSK1* null mice were profiled for this study. Mean peak-to-peak response values were statistically analyzed between mouse lines using the Student's t test, and a $p < .05$ was considered significant.

Results

MSK1 Expression and Activation in the Hippocampus

As a starting point for our analysis, we used immunohistochemical labeling to examine MSK1 expression in the hippocampus. Consistent with prior reports (Choi et al., 2012; Karelina et al., 2012), MSK1 was detected in all major neuronal cell layers, including the CA1, CA3, and the GCL (Figure 1(a)). MSK1 expression was low in the CA1 relative to expression in the CA3 and the GCL. Double immunofluorescent labeling for MSK1 and for the neuronal-specific marker NeuN (Figure 1(b)) confirmed the neuronal expression of MSK1, and double labeling with the DNA stain Hoechst showed that MSK1 was concentrated in cellular nuclei. Interestingly, although the vast majority of CA1 neurons exhibited a low level of MSK1, there was a subset of neurons that expressed high levels of the kinase (Figure 1(b): CA1 panel; arrows denote high-expressing cells). In the hilus, limited MSK1 expression was detected in NeuN-positive neurons, indicating low-level MSK1 expression in interneuron cell populations (Figure 1(b): GCL panel; boxed regions denote hilar neurons with limited MSK1 expression). MSK1 was also detected in nonneuronal cells, as noted in the CA3 panel of Figure 1(b) (arrowheads denote MSK1-positive, NeuN-negative, cells within the stratum radiatum). Finally, a *MSK1* null mouse line (Figure 1(c)) was used to test the specificity of the MSK1 immunolabeling; importantly, MSK1-like immunoreactivity (using both immunohistochemistry and Western blotting) was not detected in tissue from the *MSK1* null mouse line (Figure 1(d)).

Next, we examined MSK1 activation resulting from pilocarpine-evoked (310 mg/kg: IP injection) SE. Of note, the SE model system has been widely used to examine mechanisms of excitotoxic and neuroprotective response processes and mechanisms underlying epileptogenesis (White, 2002; Curia et al., 2008; Curia et al., 2014). Initially, mice were sacrificed 15 to 30 min after the induction of Stage 5 seizure activity, and hippocampal tissue was probed with an antibody against the Ser-360 phosphorylated form of MSK (pMSK), a marker of MSK activation (McCoy et al., 2005). Of note, this antibody does not distinguish between MSK1 and MSK2. In control, vehicle-injected mice, very limited pMSK was detected within the principal cell layers of the hippocampus, although high background staining was observed in the hippocampal subfields and fiber tracks (Figure 2(a)). In contrast, SE evoked marked MSK phosphorylation in the major hippocampal cell layers (CA1, GCL: Figure 2(b)) and in the CA3 (data not shown); this expression pattern is consistent with the nuclear expression pattern that was observed for total MSK1 expression (see Figure 1(b)). Immunohistochemistry was complemented with pMSK Western analysis of hippocampal lysates (probed with the same pMSK antibody used for

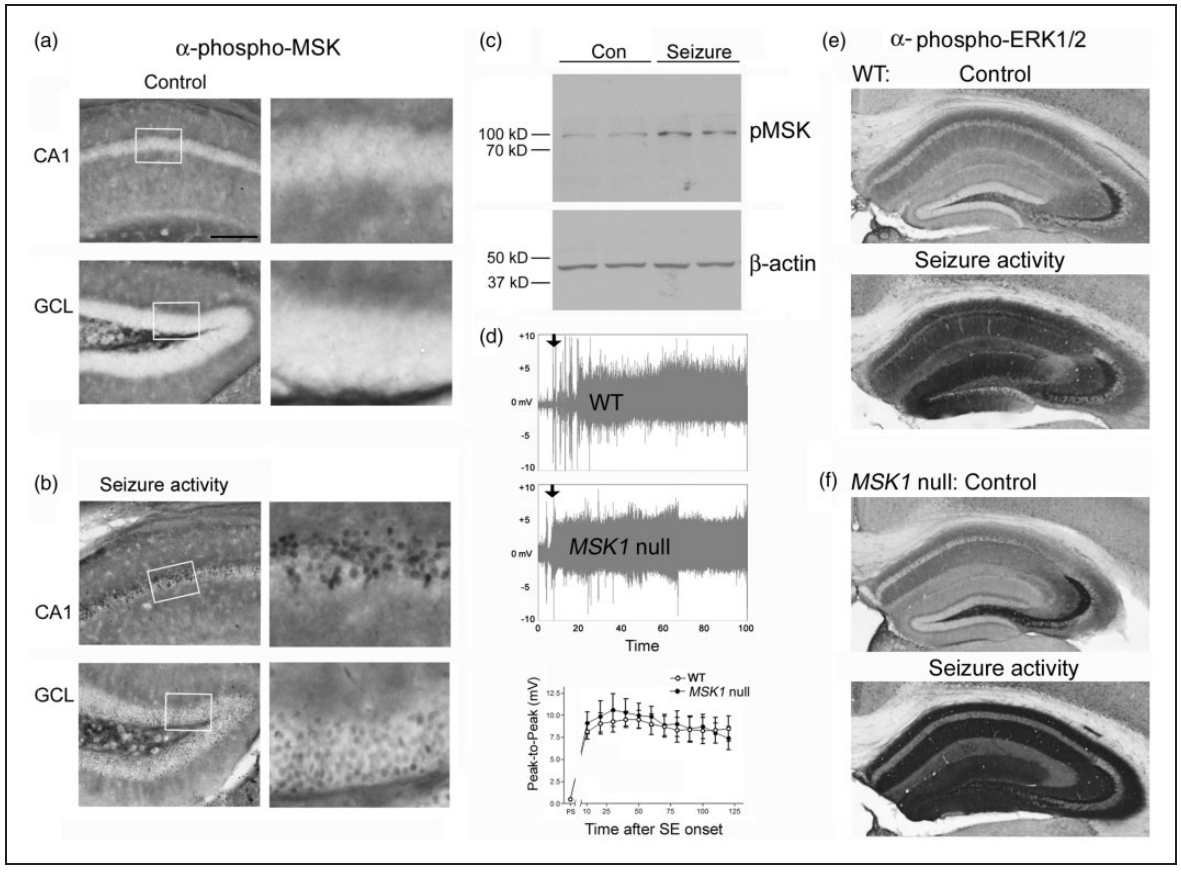

Figure 2. Seizure activity stimulates MSK activation. WT mice were injected with vehicle (control) or with pilocarpine and sacrificed 15 to 30 min after the induction of Stage 5 seizure activity. (a) Immunohistochemical labeling revealed limited MSK phosphorylation in the CA1 and GCL of control mice. (b) Marked phosphorylation in the CA1 and GCL was detected following seizure activity. Boxed regions in the left panels in (a) and (b) are magnified and presented to the right. Bar: 50 μm. (c) Western analysis of hippocampal lysates (from WT mice) were also used to profile MSK phosphorylation (pMSK) following seizure activity: Note that the increased band intensity in lysates isolated from pilocarpine (seizure)-treated animals. As a loading control, the blot was also probed for β-actin expression. Each lane represents lysate from an individual animal. Data are representative of three separate trials. (d) EEG analysis of pilocarpine-evoked SE. Top: representative traces from a WT and *MSK1* null mouse. Recordings are from the start of motor seizure activity and continue to SE. Arrows denote the approximate onset of SE. Bottom: Mean SE-evoked EEG activity amplitude (peak-to-peak: P–P) for WT and *MSK1* null mice. Significant P–P differences were not detected between the genotypes at any of the time points. Data were averaged from four animals from each genotype. Immunohistochemical labeling for ERK1/2 activation in WT (e) and *MSK1* null mice (f). Animals were sacrificed 30 min after vehicle injection (top panels) or ~15 min after pilocarpine-evoked Stage 5 seizure activity (bottom panels). Note the marked increase in seizure-evoked hippocampal ERK1/2 activation in both WT and *MSK1* null mice. Data are representative of triplicate determinations.

immunolabeling). Relative to control tissue, SE trigged an increase in the expression of an ~90 kDa band, consistent with the molecular weight of MSK1 (and MSK2). As a control, the blot was also probed for total β-actin expression. Together, these data reveal that MSK1 is expressed in hippocampal neurons, and that its activation is coupled to seizure activity.

MSK1 Confers Neuroprotection Against Excitotoxic Cell Death

Next, we examined the potential role of MSK1 signaling in the excitotoxic response induced by SE. This line of inquiry was predicated on a large body of work showing that the MSK1 effector pathways (ERK/MAPK and P38/MAPK) affect cell viability. To address this question, we used a *MSK1* null mouse line ($MSK1^{-/-}$: Figure 1(c) and (d)), in which the *MSK1* allele was selectively deleted using homologous recombination (Arthur and Cohen, 2000). In our two prior studies (Choi et al., 2012; Karelina et al., 2012), we provided a detailed description of the line, noting that *MSK1* null mice are fertile, and that no health issues were detected. Further, compared with the WT mice, gross morphological differences in the hippocampus were not detected in *MSK1* null mice. Of note, degeneration has been described within the striatum of aged (9 months) *MSK1* null mice (Martin et al., 2011). However, within the 6- to 14-week age range used in our study, hippocampal neurodegeneration was not detected (described later). Further, with respect to the SE paradigm, WT mice and *MSK1* null mice showed similar seizure onset times following pilocarpine injection, and there were no marked differences in the motor manifestations, and the progression of seizure severity. Using the Racine scale (Racine, 1972) both lines exhibited the stepwise progression from Stage 1 to Stage 5 seizure activity. A subset of *MSK1* null (35%) and WT (40%) mice transitioned to SE; SE-evoked mortality rates between the two lines were similar, with MSK1 nulls exhibiting a slightly higher rate than WT mice (45% vs. 40%, respectively, $N = 20$/per genotype). EEG recording revealed high-amplitude electrical discharges, and peak-to-peak analysis detected a similar level of SE-evoked electrical activity in WT and *MSK1* null mice (Figure 2(d)). Finally, immunohistochemical labeling for the activated, dual phosphorylated, form of ERK1/2 was used to test whether seizure activity drives an expected increase in ERK/MAPK pathway activation. In both WT (Figure 2(e)) and *MSK1* null (Figure 2(f)) lines, 15 min of Stage 5 seizure activity led to a robust, hippocampal wide, increase in ERK phosphorylation. Together, these data indicate that *MSK1* null and WT mice exhibit similar sensitivities and response properties to pilocarpine. Further, when combined with the data described later, these results indicate that the *MSK1* null cell death phenotype is likely not the result of an enhanced sensitivity to pilocarpine, but rather can be ascribed to an elevated cellular-level vulnerability to the excitatory insult.

To analyze the potential role of MSK1 in SE-evoked excitotoxic cell death, WT (referred to as $MSK1^{+/+}$ mice in the figure) and MSK1 null mice were sacrificed 3 days after pilocarpine-evoked SE, and hippocampal tissue was examined for cell death via FJB labeling. Initially, under control conditions (no pilocarpine injection), FJB-positive cells were not detected in the WT or *MSK1* null mice (Figure 3(a)–(d)). In WT mice, SE led to cell death within the CA1, CA3, and hilar region, whereas limited cell death was detected in the GCL (Figure 3(a)). Interestingly, compared to WT mice, *MSK1* null mice exhibited a significant increase in SE-evoked cell death within the CA1 and CA3 cell layers (Figure 3(a)–(c)). However, within the hilus, similar high levels of cell death were detected in WT and *MSK1* null mice (Figure 3(a) and (d)).

Nissl staining was used to complement the 3-day post-SE FJB labeling and extend the analysis of cell death out to 6-week post-SE (Figure 4)—a time point when animals exhibit spontaneous seizure activity. Nissl staining of tissue at the 3-day post-SE time point confirmed the findings using FJB: A significant increase in CA1 and CA3 cell death in *MSK1* null mice relative to WT mice (Figure 4(a) and (c)). Interestingly, marked degeneration of the GCL was observed in 1 *MSK1* null mice (Figure 4(a), bottom panel), which represents ~6% of the *MSK1* null mice profiled ($n = 18$ in total); GCL degeneration was not detected in WT mice ($n = 20$ in total). Representative data and quantitative analysis for the 6-week time point revealed a significantly higher level of cell death in the *MSK1* null line (Figure 4(b)–(d)). Together, these data indicate that MSK1 confers potent neuroprotection against SE-evoked excitotoxicity. Further, these data indicate that the abrogation of MSK1 signaling does not affect cell viability under normal, nonpathophysiological conditions. Here, it is worth noting that a prior study reported that MSK1 enhances neuronal cell death (Hughes et al., 2003). Clearly, this result is inconsistent with our work reported here. Possible explanations for these divergent results could be related to either the experimental methods used to stimulate an excitotoxic challenge or the different experimental methods used to disrupt MSK1 signaling (the work of Hughes et al. largely utilized small molecular inhibitor-based approaches). As noted in the Introduction section, signaling via the ERK/MAPK pathway can confer neuroprotection or facilitate neuronal cell death, depending on the stimulus conditions: Given that MSK1 is downstream of ERK/MAPK, it may also play a similar, context-specific, role.

The increase in evoked cell death observed in *MSK1* null mice could be due to a number of factors, including

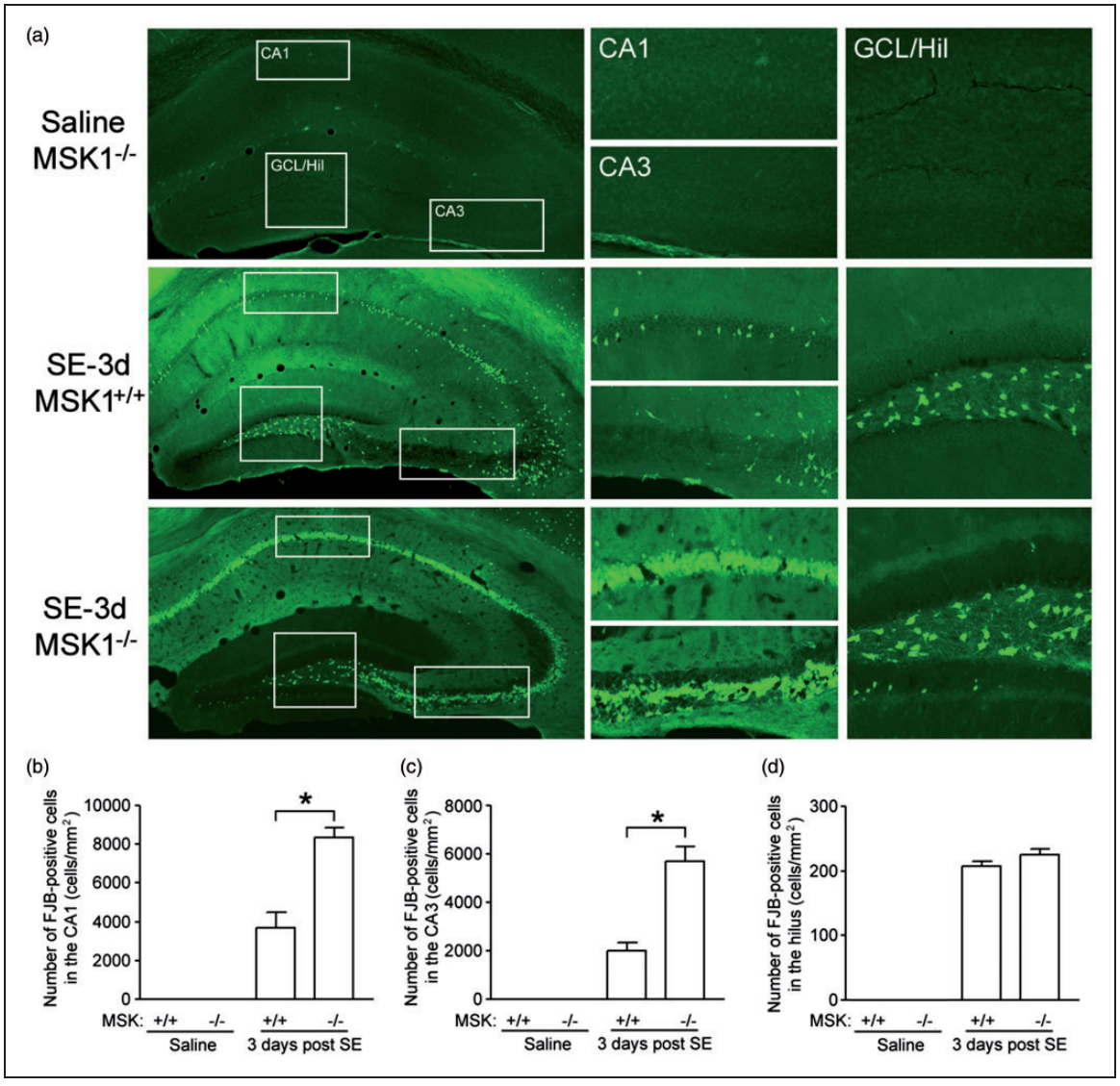

Figure 3. SE-evoked cell death phenotype in *MSK1* null mice. (a) *MSK1* null mice (MSK1$^{-/-}$) and WT (MSK1$^{+/+}$) mice were challenged with pilocarpine-evoked SE (or saline vehicle), sacrificed 3 days later, and coronal sections through the hippocampus were labeled with FJB. In WT mice, SE evoked a stereotypical pattern of cell death in the hilus, CA3, and CA1 cell layers. Interestingly, in *MSK1* null animals, there was a marked, relative, increase in cell death within the CA3 and CA1 cell layers. ((b)–(d)) Quantitative analysis of FJB-positive cells in the CA1 (b), CA3 (c), and hilus (d). *$p < .01$. Of note, in control mice (saline injection), cell death was not detected in either *MSK1* null or WT mice.

an increase in SE-evoked excitatory drive and a decrease in cellular neuroprotection. To address these two possibilities, we prepared primary hippocampal neuronal cultures from postnatal day 1 *MSK1* null and WT mice and tested their response profiles to NMDA stimulation. We initially tested NMDA-induced cell death in neurons cultured for 10 days using the LDH assay. For these studies, neurons were stimulated (20 min) with 50 μM NMDA (supplemented with 2-μM glycine), and LDH release was examined 4 h and 8 h later. Relative to WT neurons, NMDA-evoked cell death was markedly increased in *MSK1* null cultures at both time points (Figure 5(a)). Photomicrographs of *MSK1* null cultures at 8 h post-NMDA stimulation revealed a large number of shrunken cells with fragmented processes; in contrast, the cellular morphology of WT neurons was largely intact, with only a relatively small number of cells exhibiting signs of necrosis (Figure 5(b)). To confirm that cell death occurred in neurons, cultures were also labeled for the neuronal-specific cytoskeletal protein MAP2, which has been used to profile excitotoxic cell death in culture (Carrier et al., 2006). Consistent with the LDH data set, *MSK1* null cultures treated with NMDA showed a reduction in MAP2 labeling relative to the control *MSK1* null

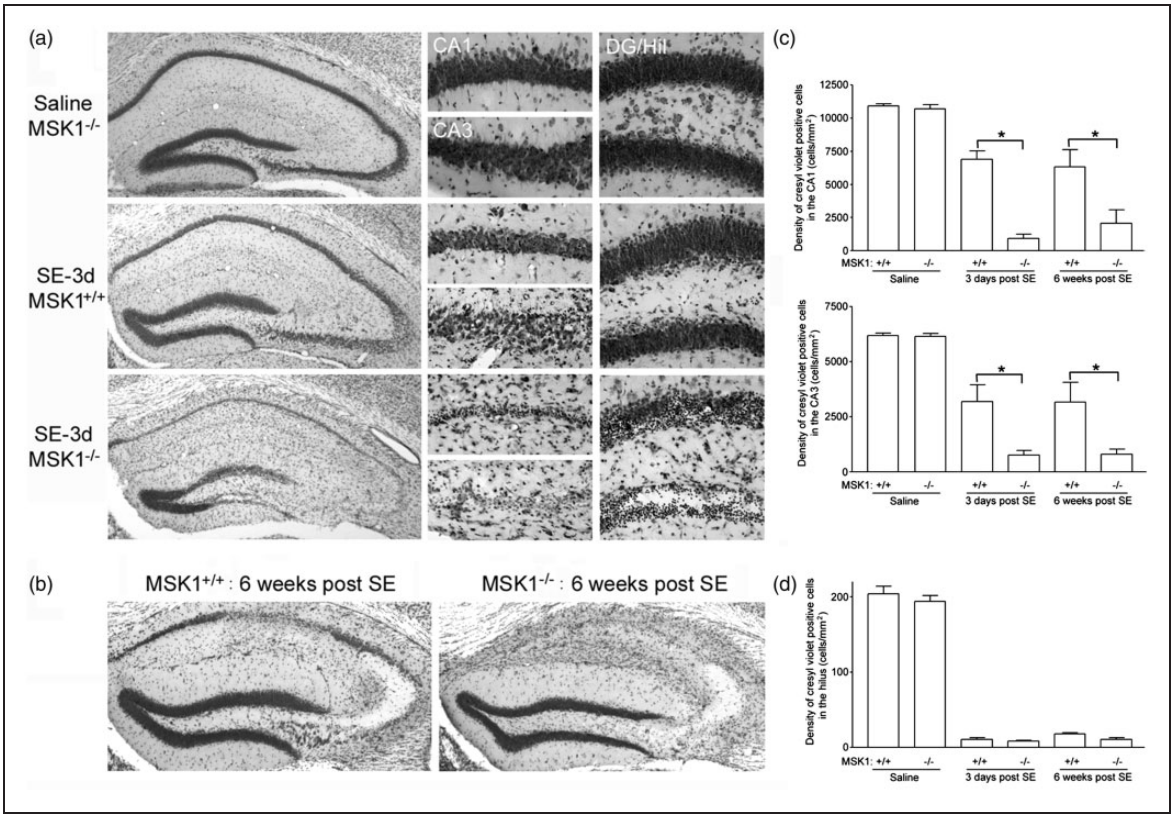

Figure 4. Cell death at 3 days and 6 weeks post-SE. Nissl staining was used to profile SE-induced cell death in WT (MSK1$^{+/+}$) and *MSK1* null (MSK1$^{-/-}$) mice. (a) Consistent with the cell death profile generated using FJB labeling (Figure 3), an elevated level of cell death was detected in the CA1 and CA3 cell layers of *MSK1* null mice at the 3-day post-SE time point. Interestingly, marked cell death was occasionally observed in the GCL layer of *MSK1* null mice. (b) Representative Nissl staining at 6 weeks post-SE in WT and *MSK1* null mice; note the marked cell death within the CA1 and CA3 cell layers of *MSK1* null mouse Quantitation of cell density in the CA1 and CA3 (c) and the hilar (d) cell layers at both the 3-day and 6-week post-SE time points. *$p < .01$.

cultures (mock stimulation) and compared to WT cultures treated with NMDA (Figure 5(c)). Together, these data indicate that MSK1 contributes to cell-autonomous neuroprotective response mechanisms.

To extend this line of work, we also examined NMDA-evoked calcium responses of *MSK1* null neurons. For these studies, neurons were cultured for 10 days, loaded with the calcium-sensitive fluorophore Fura-2, and the response profiles of individual neurons were monitored following brief (~30 s) treatments with NMDA (10–100 μM). Surprisingly, the peak-evoked responses to NMDA were significantly lower in the *MSK1* null neurons than in WT neurons (Figure 6(a) and (b)). Near the end of the experiment (Figure 6(a)), neurons were exposed to 100 μM NMDA for 5 min; this long stimulus paradigm was used to assess whether the response profiles to chronically elevated Ca^{2+} levels were affected by MSK1 deletion. Compared to the WT cells, *MSK1* null neurons exhibited a significantly reduced average response profile to the chronic Ca^{2+} load (Figure 6(c)). Of note, basal calcium levels were significantly higher in MSK1 null neurons compared to WT neurons (Figure 6(d)). Collectively, the cellular level analysis presented here indicates that the disruption of MSK1 signaling reduces excitatory drive, while increasing vulnerability to potentially excitotoxic stimuli.

MSK1 Deletion Alters the Hippocampal Transcriptome

Finally, the complex nature of the MSK1 cell death phenotype (reduced excitatory drive, elevated excitotoxic response to NMDA, and elevated SE-evoked cell death) led us to explore the contribution of MSK1 to the hippocampal transcriptional profile. To this end, hippocampal RNA was isolated from WT and *MSK1* null mice and profiled via Affymetrix array (all array data are presented in a Supplemental Excel Spreadsheet). Using a 1.25-fold cutoff, and a p value of $< .05$, our data set revealed that the disruption of MSK1 reduced the expression of 130 genes and increased the expression of 145 genes (Figure 7(a) and Table 1). Gene ontology (GO) functional clustering analysis via the Database for Annotation, Visualization and Integrated Discovery (DAVID) revealed that

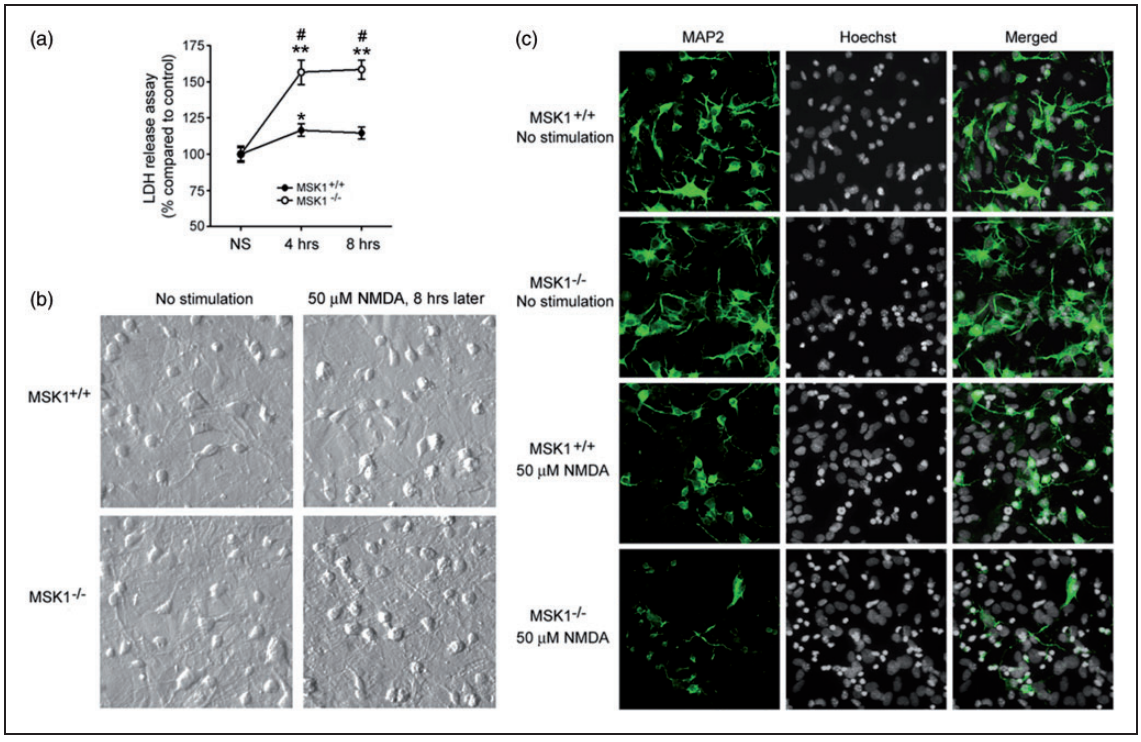

Figure 5. NMDA-evoked cell death in cultured hippocampal neurons. (a) Primary hippocampal neuronal cultures of *MSK1*$^{-/-}$ null and MSK1 WT (MSK1$^{+/+}$) tissue were maintained for 10 days and then stimulated with NMDA (50 μM with 2 μM glycine added: 20 min), and LDH release was profiled 4 h and 8 h later. Relative to no stimulation, NMDA evoked a modest increase in LDH release in WT neurons. In contrast, marked cell death was detected in MSK1 null neurons. *$p < .05$ relative to the control, no stimulation, condition; **$p < .01$ relative to the control, no stimulation, condition; #$p < .01$ comparing LDH release between the *MSK1* null and WT cultures for each time point. Mean data points were generated from quadruplicate determinations. (b) Representative images of cultured neurons under control conditions (no stimulation) and 8 h after NMDA stimulation. For the NMDA-treated condition, note the relatively large number of *MSK1* null neurons with condensed cell bodies and fragmented processes. (c) Cell viability following NMDA receptor stimulation was also assayed via MAP2 immunolabeling and nuclear staining with Hoechst. Again, note the relative increase in the number of condensed nuclei and the loss of MAP2 labeling in *MSK1* null neurons at 8 h after NMDA treatment.

MSK1 deletion had significant effects on the expression of several classes of genes associated with membrane receptor signaling, cytoskeletal organization, and redox chemistry (Figure 7(b)). The GO term *Neuronal Apoptosis* exhibited clustering, although significance was just below the $p < .05$ cutoff (Figure 7(b)). Together, these data indicate that MSK1 regulates the expression of a large number of genes that underlie basic cellular biochemistry and neuronal-specific cellular signaling.

Discussion

Here, we provide evidence supporting a role for MSK1 as a critical component of a neuroprotective response pathway that limits cell death resulting from SE. Using a 3-day post-SE time point, we observed extensive cell death in the CA1, CA3, and hilar regions of the hippocampus and relatively modest cell death in the GCL. This cell death pattern is consistent with an extensive literature on pilocarpine-evoked cell death (Olney et al., 1983; Freund et al., 1992; Borges et al., 2003; Zhang et al., 2009; Tang and Loke, 2010). Further, this pattern of cell death was largely intact in *MSK1* null mice; hence, MSK1 did not consistently confer vulnerability to any additional cell types; rather, the loss of MSK1 exacerbated cell death in inherently vulnerable cell populations (i.e., pyramidal neurons of CA1 and CA3 cell layers). Interestingly, cell death in the hilus was not affected in *MSK1* null mice. One possible explanation for this is that SE has been shown to trigger very high levels of hilar interneuron cell death (Buckmaster and Dudek, 1997; Choi et al., 2007; Sun et al., 2007), and thus, this high degree of cell death could preclude any effects of *MSK1* deletion. However, it is also worth noting that our immunofluorescent labeling revealed limited MSK1 expression in hilar neurons. Could this limited expression of MSK1 in hilar neurons contribute to their inherently high level of sensitivity to SE? Clearly, further studies that focus on hilar interneurons and MSK1 signaling will be needed to address this idea. As noted above, the GCL is relatively resistant to the excitotoxic effects of pilocarpine-evoked SE (Olney et al., 1983; Freund et al., 1992; Cavazos et al., 1994; Mori et al., 2004). Given the

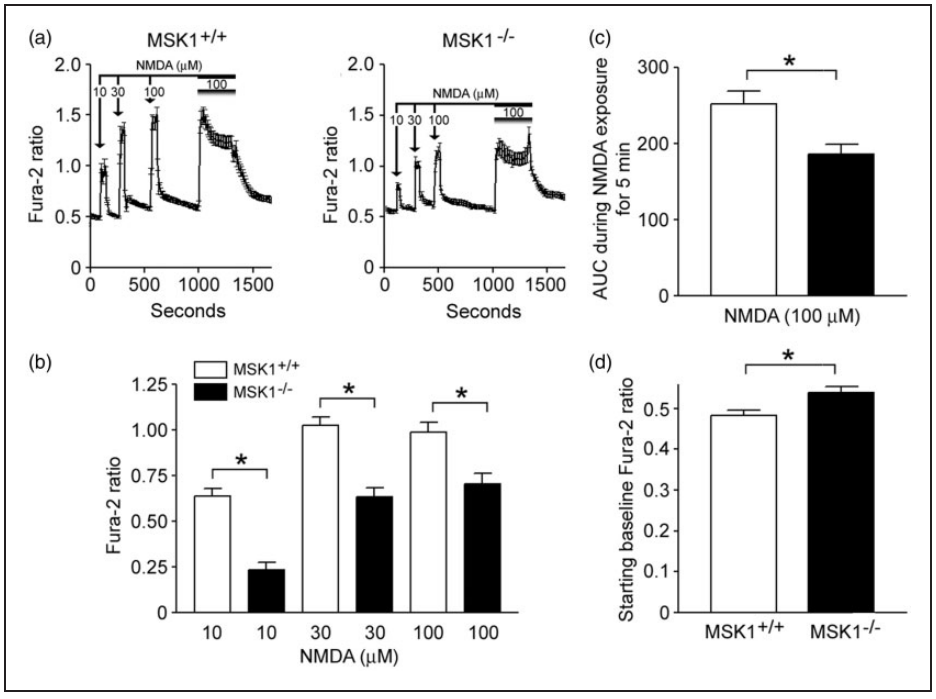

Figure 6. Evoked Ca^{2+} influx is reduced in *MSK1* null neurons. (a) Primary neuronal cultures were maintained for 10 days, loaded with Fura-2, and evoked Ca^{2+} influx was profiled following sequential administrations of NMDA (10, 30, and 100 μM: 30 s each; followed by 100 μM for 5 min). (b) Data represent the mean and SEM of WT ($MSK1^{+/+}$) cultures and $MSK1^{-/-}$ null cultures. (c) Average Ca^{2+} response evoked with 100 μM NMDA exposure for 5 min expressed as the mean area under the curve (AUC) for each genotype. (d) Mean resting Ca^{2+} level recorded at the beginning of the experiment. *$p < .05$. Data were averaged from 29 neurons from the *MSK1* null cultures and 43 neurons from the MSK1 WT cultures.

high level of MSK1 expressed in the GCL, we speculated that *MSK1* null mice could exhibit GCL vulnerability to SE. However, the data presented here showed that *MSK1* deletion did not consistently enhance GCL neuronal sensitivity to SE (of note, we did observe that one out of 18 *MSK1* null animals showed marked SE-evoked GCL degeneration, see Figure 4(a)). These data coupled with the data from the CA1 and CA3 cell layers indicate that factors working independently of the MSK1 signaling network regulate SE-evoked cell death in the GCL layer of the hippocampus.

Here, we detected robust inducible MSK1 phosphoactivation in response to seizure activity, and that under control conditions, MSK1 activation was relatively low throughout the hippocampus. This pattern of robust SE-evoked MSK1 activity is consistent with work showing that the ERK/MAPK and P38 pathways (the two upstream effectors of MSK1) are activated following multiple seizure induction paradigms in the hippocampus (Baraban et al., 1993; Gass et al., 1993; Kim et al., 1994; Garrido et al., 1998; Jiang et al., 2005; Choi et al., 2007; Lopes et al., 2012). This dynamic, inducible, activation of MSK1 raises a question: Is SE-evoked MSK1 activity required to confer neuroprotection or is the tonic, basal level of MSK1 activity sufficient to drive neuroprotection. As noted earlier, Martin et al. (2011) reported striatal deterioration in aged MSK1 null mice. This finding could be used to support the idea that the disruption of basal MSK1 activity is sufficient to drive vulnerability to stressful stimuli. However, it is also worth noting that a number of studies have shown that the disruption of basal ERK/MAPK activity does not affect cell health, but rather leads to the abrogation of an evoked neuroprotective response (Han and Holtzman, 2000; Kuroki et al., 2001; Pedersen et al., 2002; Park et al., 2004; Nguyen et al., 2005). Hence, it is likely that both basal and stress-evoked MSK1 signaling contribute to the neuroprotective response. Here, it is also worth noting that *MSK1* deletion did not affect hippocampal neuronal cell viability under normal physiological conditions. Rather, the *MSK1* null cell death phenotype was only revealed under stress conditions. In some respects, this is consistent with studies showing that the disruption of CREB (a downstream MSK1 target) does not, by itself, trigger cell death, but does increase neuronal vulnerability to excitatory insults (Lee et al., 2005; Lee et al., 2009). Notably, as with CREB, MSK1 has been implicated in a range of plasticity-dependent processes, including learning and memory, and activity dependent synapse formation (Chwang et al., 2007; Corrêa SA et al., 2012; Karelina et al., 2012). Together, these data indicate that MSK1 plays at least two distinct roles in the central nervous

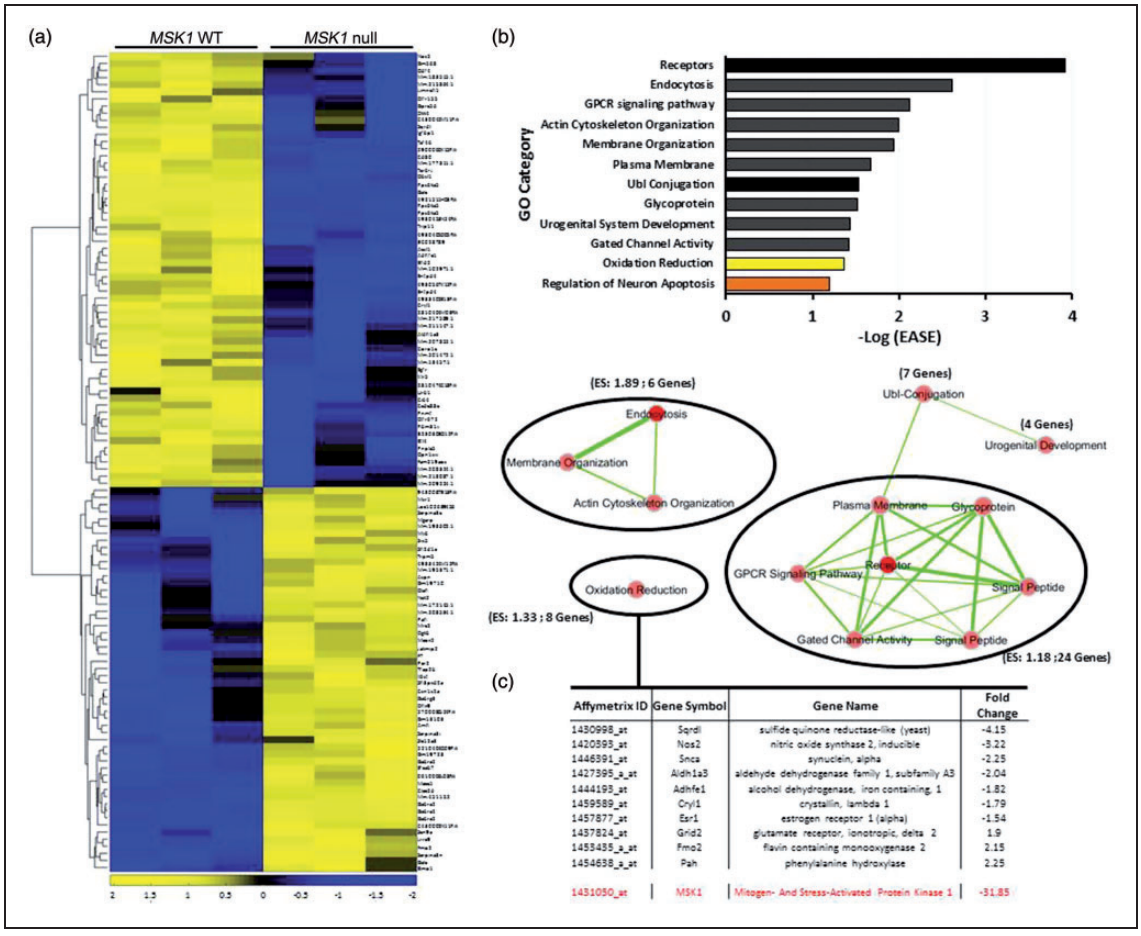

Figure 7. Hippocampal gene expression profile of *MSK1* null mice. (a) Hierarchical cluster analysis comparing differentially expressed genes between MSK1 WT and *MSK1* null mice. A total of 275 genes showed significant changes ($\geq$1.25-fold) in expression, with 145 genes upregulated and 130 genes downregulated. ((b), Top) DAVID functional annotation chart showing enriched gene ontology categories. Top, Categories are sorted based on the EASE score ($p < .05$). ((b), Bottom) Functional annotation clustering output from DAVID is represented using the Enrichment Map application from Cytoscape. The Enrichment Score (ES) and the number of genes are specified for each cluster. (c) List of genes corresponding to the DAVID Oxidation Reduction Annotation Cluster. As a confirmation of the effectiveness of the Array profiling, the fold-reduction in *MSK1* expression is noted using red font.

system: one that couples synaptic activity to changes in functional plasticity and a second role as an effector of neuroprotective signaling. Further work will be required to determine the relative contribution of CREB to the neuroprotective effects elicited by MSK1 signaling.

Given the enhanced cell death phenotype, it was surprising to find that *MSK1* null neurons exhibited weaker NMDA-evoked excitatory drive compared to WT neurons, as assessed using Ca^{2+} imaging. Interestingly, reduced excitability may be consistent with studies showing that *MSK1* null mice exhibit reduced functional plasticity, including activity-dependent spine formation, synaptic scaling, and cognition (Chwang et al., 2007; Corrêa SA et al., 2012; Karelina et al., 2012). Further, the weak-evoked Ca^{2+} response in *MSK1* null neurons indicates that the enhanced cell death phenotype likely cannot be ascribed to aberrant excitatory drive. Rather, these data point to the compromised expression of neuroprotective genes and gene networks in *MSK1* null neurons.

Could the enhanced SE-evoked cell death in *MSK1* null mice result from dysregulated apoptotic and necrotic cell death mechanisms? With respect to apoptosis, extensive work in nonneuronal cells has shown that MSK regulates cell survival via the regulation of antiapoptotic cell death mechanisms (Mu et al., 2005; Kannan-Thulasiraman et al., 2006; Dumka et al., 2009; Joo and Jetten, 2010; Odgerel et al., 2010; Healy et al., 2012; Moens and Kostenko, 2013), including the regulation of NF-κB, BAD, and caspase activation (She et al., 2002; El Mchichi et al., 2007). Further, the CREB/CRE transcriptional pathway, a principal target of MSK1, has also been shown to regulate apoptotic cell death (reviewed in Sakamoto et al., 2011).

In contrast to the extensive work on MSK and apoptotic cell death, to our knowledge, limited work has

explored the potential contribution of MSK signaling to necrotic cell death. Necrotic cell death is typically associated with elevated intracellular Ca^{2+} levels, rapid ATP depletion, and mitochondrial swelling; these and other events lead to the collapse of the membrane potential and the rupturing of the plasma membrane. Although our data did not identify an effect of MSK1 deletion on Ca^{2+} homeostatic, or evoked responses, our array data indicate that MSK1 regulates the expression of several genes that could affect neuronal vulnerability. Many of these genes are associated with oxidation/reduction chemistry (*alcohol dehydrogenase*, *phenylalanine hydroxylase*, *NOS2*, *sulfide quinone reductase*) and membrane receptor signaling (*epidermal growth factor receptor*, *GABA-A receptor subunit alpha 2*) and cellular transport (e.g., *alpha-synuclein*, *EHD2*, *coronin*).

Interestingly, one of the strongest effects of MSK1 deletion was on the expression of galactosylceramidase (Galc): ~14-fold decrease in expression. Galc is highly expressed in both neurons and oligodendrocytes and serves as a key enzyme in the metabolism of galactolipids. Loss-of-function mutations in Galc underlie the development of Krabbe disease in humans (Wenger et al., 2000). Interestingly, the *Twitcher* mouse line (a model of Krabbe disease) bred onto a C57BL/6J and 129SvEv mixed background shows spontaneous neuronal cell death within the hippocampus (Tominaga et al., 2004). These observations raise the prospect that reduced Galc expression in *MSK1* null mice may also contribute to the cell death phenotype reported here. However, it is worth noting that the developmental and motor phenotypes associated with the *Twitcher* line (i.e., stunted growth, twitching and limb weakness reported by Duchen et al. (1980)) were not observed in the *MSK1* null line. Clearly, the list of genes that are regulated by MSK1 is extensive, and as such, the cell death phenotype observed here could have resulted from a complex interplay of affected genes and gene networks. It is also worth noting that the effects of *MSK1* deletion on cell type-specific neuroprotective genes may have evaded detection, given that the whole hippocampus was used for our array profiling.

In conclusion, the data reported here reveal that MSK1 regulates neuroprotective signaling in the CA1 and CA3 sublayers of the hippocampus. This effect occurs on a cellular level and is not associated with increased cellular excitability. These findings justify further work examining the potential role of MSK1 in other mechanisms of cell stress and neuroprotection, including ischemia and preconditioning. Finally, the elevated levels of cell death observed in *MSK1* null mice raise the prospect that approaches designed to enhance MSK1 activity could abrogate some of the pathophysiological effects associated with, and potentially underlying, the development of epilepsy.

Table 1. Microarray Significant Results.

Probe set	Gene	Accession	Entrez Gene	Description	WT-1	WT-2	WT-7	Baseline mean	Baseline mean's SE	MSK-14	MSK-15	MSK-9	Experiment mean	Experiment mean's SE	Fold change	*t* statistic	*p* value
1431050_at	Rps6ka5: ribosomal protein S6 kinase, polypeptide 5	BE291900	73086	Mm.39471.1	247.85	229.11	261.03	246.24	9.96	9.86	8.49	5.6	7.73	2.76	−31.85	−23.074	.000889
1440343_at	Rps6ka5: ribosomal protein S6 kinase, polypeptide 5	BQ174267	73086	Mm.31856.1	433.39	363.13	431.32	409.11	23.65	18.13	23.67	25.32	22.18	4.6	−18.44	−16.063	.002803
1452907_at	Galc: galactosylceramidase	AK010101	14420	Mm.141399.1	438.54	447.84	455.13	447.9	9.59	30.14	31.64	31.49	31.08	9.41	−14.41	−31.024	.000006
1422360_at	Olfr672: olfactory receptor 672	NM_020292	258755	Mm.103736.1	6.76	7.4	8.18	7.59	1.12	1	2.14	1.59	1.38	1.16	−5.51	−3.852	.018297
1429511_at	4933402E13Rik: RIKEN cDNA 4933402E13 gene	AK016614	74437	Mm.85792.1	14.46	23.85	13.78	17.35	3.41	5.88	1.74	2.39	3.74	1.68	−4.63	−3.574	.039174
1446525_at	Mm.217589.1	BM198842		Mm.217589.1	10.59	11.88	6.92	9.89	2.05	3.54	1	2.48	2.19	1.02	−4.51	−3.368	.04488
1420251_at	Mm.177311.1	AV172782		Mm.177311.1	14.11	8.21	9.8	10.83	1.89	3.04	2.16	2.39	2.56	0.65	−4.23	−4.14	.036928
1444813_at	Mm.211147.1	BB521324		Mm.211147.1	13.49	15.02	12.45	13.82	1.83	5.04	1	4.28	3.3	1.64	−4.19	−4.285	.013115

(continued)

Table 1. Continued

Probe set	Gene	Accession	Entrez Gene	Description	WT-1	WT-2	WT-7	Baseline mean	Baseline mean's SE	MSK-14	MSK-15	MSK-9	Experiment mean	Experiment mean's SE	Fold change	*t* statistic	*p* value
1430998_at	Sqrdl: sulfide quinone reductase-like (yeast)	BE626283	59010	Mm.28986.2	13.44	16.58	9.47	13.42	2.4	2.01	6.52	1.38	3.23	2.29	−4.15	−3.072	.037307
1460269_at	Pnmt: Phenylethanolamine-N-methyltransferase	AV380429	18948	Mm.213024.1	4.34	5.7	6.69	5.47	1.01	1	1.79	1.84	1.38	1.04	−3.97	−2.828	.047481
1432739_at	2900060K15Rik: RIKEN cDNA 2900060K15 gene	AV154271	73041	Mm.158931.1	3.14	4.73	2.84	3.57	0.61	1	1.02	1.06	1.02	0.65	−3.51	−2.852	.046521
1428038_at	Gm568: predicted gene 568	BC028561	230143	Mm.34995.1	10.89	15.26	9.71	12.09	2.04	6.25	4.33	1	3.61	1.84	−3.35	−3.087	.037174
1457878_at	C430042M11Rik: RIKEN cDNA C430042M11 gene	BB415623	320021	Mm.187012.1	13	14.01	14.28	13.86	1.21	2.37	8.55	1.58	4.2	2.53	−3.3	−3.449	.04372
1420393_at	Nos2: nitric oxide synthase 2, inducible	AF065921	18126	Mm.2893.1	28.03	22.19	16.26	22.22	3.46	14.06	5.8	1	6.91	3.83	−3.22	−2.969	.041706
1443153_at	Trip11: Thyroid hormone receptor interactor 11	BB306866	109181	Mm.208618.1	50.29	67.54	79.11	65.85	8.95	21.82	24.58	18.55	21.83	3.22	−3.02	−4.626	.027847
1444388_at	Mm.183515.1	BB020727		Mm.183515.1	7.62	8.41	7.68	8.01	1.28	3.1	3.78	1.01	2.65	1.32	−3.02	−2.917	.043423
1457563_at	Egfr: epidermal growth factor receptor	BB409522	13649	Mm.209083.1	16.68	14.27	11.08	14.12	1.9	4.3	4.47	8.39	5.75	1.78	−2.45	−3.217	.032562
1452205_x_at	Gm6273 /// LOC381765 /// LOC665506 /// Tcrb-J: predicted gene 6273 /// similar to T cell antigen receptor /// similar to T-cell receptor beta-2 chain C region /// T-cell receptor beta, joining region	X67128	21580 /// 381765 /// 621968 /// 665506	Mm.157012.8	16.19	12.54	12.85	14.04	2.24	6.17	5.43	5.78	5.76	1.86	−2.44	−2.844	.048518
1427717_at	Cd80: CD80 antigen	X60958	12519	Mm.89474.7	13.12	12.49	10.69	12.18	1.37	5.72	4.5	5.23	5.01	1.44	−2.43	−3.606	.022721
1447355_at	Acsl1: acyl-CoA synthetase long-chain family member 1	BQ128552	14081	Mm.220877.1	18.29	14.71	17.72	17.17	1.32	9.01	7.64	5.43	7.32	1.36	−2.35	−5.196	.006558
1432542_at	2810474C18Rik: RIKEN cDNA 2810474C18 gene	AK013405	72785	Mm.158882.1	15.84	14.47	14.31	14.89	1.45	4.75	5.65	8.84	6.43	1.67	−2.32	−3.829	.01929
1418918_at	Igfbp1: insulin-like growth factor binding protein 1	NM_008341	16006	Mm.21300.1	20.88	22.01	18.16	20.54	1.95	8.59	10.66	7.29	9.12	1.94	−2.25	−4.152	.014233
1446391_at	Mm.209224.1	BB450769		Mm.209224.1	46.08	37.53	38.56	40.36	3.07	6.88	23.35	23.45	17.98	6.06	−2.25	−3.297	.046654

(continued)

Table 1. Continued

Probe set	Gene	Accession	Entrez Gene	Description	WT-1	WT-2	WT-7	Baseline mean	Baseline mean's SE	MSK-14	MSK-15	MSK-9	Experiment mean	Experiment mean's SE	Fold change	*t* statistic	*p* value
1453330_at	Ccdc88c: coiled-coil domain containing 88C	AK002458	68339	Mm.45291.1	73.53	68	94.64	78.69	9.05	25.48	43.19	43.47	37.06	8.27	−2.12	−3.394	.027765
1425447_at	Dkk4: dickkopf homolog 4 (Xenopus laevis)	BC018400	234130	Mm.157322.1	11.78	13.87	14.1	13.31	1.32	5.66	9.64	3.76	6.33	1.91	−2.1	−3.003	.046368
1427395_a_at	Aldh1a3: aldehyde dehydrogenase family 1, subfamily A3	BC026667	56847	Mm.140988.2	11.52	10.4	9.43	10.6	1.01	5.46	2.55	6.98	5.19	1.49	−2.04	−2.996	.04721
1443483_at	Xlr5a /// Xlr5b /// Xlr5c: X-linked lymphocyte-regulated 5A /// X-linked lymphocyte-regulated 5B /// X-linked lymphocyte-regulated 5C	BM207672	27084 /// 574438 /// 627081	Mm.139096.1	21.31	20.23	16.11	19.43	2.21	6.87	8.68	13.61	9.85	2.41	−1.97	−2.93	.043207
1454248_at	Cib4: calcium and integrin binding family member 4	AK006670	73259	Mm.158977.1	16.11	19.23	21.9	19.13	2.24	7.79	9.06	12.46	9.9	1.81	−1.93	−3.199	.034969
1457121_at	Obsl1: obscurin-like 1	AV271877	98733	Mm.213076.1	21.54	20.84	20.23	20.81	2.1	10.39	9.88	11.95	10.76	2.16	−1.93	−3.342	.028807
1431887_at	Rbm31y: RNA binding motif 31, Y-linked	AK017055	74484	Mm.159220.1	34.62	33.63	35.83	34.56	1.39	13.36	22.36	18.07	17.98	2.84	−1.92	−5.237	.01467
1440776_at	Limch1: LIM and calponin homology domains 1	BB709234	77569	Mm.208624.1	11.7	10.5	7.94	10.21	1.34	5.93	5.8	4.01	5.3	0.97	−1.92	−2.964	.046541
1439004_at	Rps6ka5: ribosomal protein S6 kinase, polypeptide 5	BE946999	73086	Mm.101475.1	127.44	116.07	122.49	121.67	5.29	64.56	67.62	62.11	64.78	7.26	−1.88	−6.333	.004286
1432163_at	4930567K12Rik: RIKEN cDNA 4930567K12 gene	AK016242	75845	Mm.159601.1	23.4	23.64	32.68	26.5	3.31	18.48	11.82	11.18	14.17	2.61	−1.87	−2.925	.045943
1422343_at	Olfr155: olfactory receptor 155	NM_019473	29845	Mm.88841.1	12.91	9.43	12.05	11.48	1.23	6.21	7.71	4.71	6.27	1.23	−1.83	−2.996	.040101
1420538_at	Gprc5d: G protein-coupled receptor, family C, group 5, member D	NM_053118	93746	Mm.49902.1	13.12	13.68	15.35	13.92	1.23	7.67	10.03	5.62	7.64	1.72	−1.82	−2.964	.046891
1444193_at	Adhfe1: alcohol dehydrogenase, iron containing, 1	BB177678	76187	Mm.131262.1	21.86	18.92	23.07	21.12	1.41	13.65	11.72	10.32	11.58	1.33	−1.82	−4.91	.008053
1459589_at	Cryl1: crystallin, lambda 1	C85932	68631	Mm.200251.1	14.31	11.87	11.47	12.55	0.89	8.62	5.37	6.99	7	0.93	−1.79	−4.314	.012568
1437721_at		BB543398	23790	Mm.200372.4	20.11	17.98	17.18	18.24	1.98	10.29	7.75	12.13	10.26	1.88	−1.78	−2.927	.043103

(continued)

Table 1. Continued

Probe set	Gene	Accession	Entrez Gene	Description	WT-1	WT-2	WT-7	Baseline mean	Baseline mean's SE	MSK-14	MSK-15	MSK-9	Experiment mean	Experiment mean's SE	Fold change	*t* statistic	*p* value
	Coro1c: coronin, actin binding protein 1C																
1430693_at	Pnpla5: patatin-like phospholipase domain containing 5	AV250770	75772	Mm.159565.1	52.38	49.76	43	48.13	3.46	20	37.16	24.42	27.24	5.77	−1.77	−3.104	.04719
1431193_at	Taf4b: TAF4B RNA polymerase II, TATA box binding protein (TBP)-associated factor	AK012135	72504	Mm.158836.1	29.82	37.11	29.6	32.26	2.73	19.26	18.07	16.99	18.19	1.84	−1.77	−4.278	.017046
1449190_a_at	Entpd4 /// LOC100048085: ectonucleoside triphosphate diphosphohydrolase 4 /// similar to ectonucleoside triphosphate diphosphohydrolase 4	NM_026174	100048085 /// 67464	Mm.20806.1	1825.03	1840.45	2179.94	1947.89	118.91	1355.9	1020.69	982.16	1119.68	118.27	−1.74	−4.938	.007827
1438553_x_at	4930453N24Rik: RIKEN cDNA 4930453N24 gene	BB817087	67609	Mm.105351.1	175.4	183.43	195.83	185.19	6.98	105.24	108.98	106.53	106.84	4.37	−1.73	−9.51	.001529
1438177_x_at	Entpd4 /// LOC100048085: ectonucleoside triphosphate diphosphohydrolase 4 /// similar to ectonucleoside triphosphate diphosphohydrolase 4	AV255351	100048085 /// 67464	Mm.20806.3	1188.25	1260.97	1525.79	1325.53	103.56	949.11	619.41	740.27	769.29	96.15	−1.72	−3.936	.017192
1457944_at	Mm.215864.1	BM218086		Mm.215864.1	111.91	150.14	112.66	124.95	13.14	79.86	76.75	52.04	72.57	11.43	−1.72	−3.007	.040656
1432514_at	1700066J24Rik: RIKEN cDNA 1700066J24 gene	AK006904	76992	Mm.159820.1	36.72	38.09	29.26	34.68	3.08	13.82	26.24	20.59	20.3	3.92	−1.71	−2.882	.047931
1457653_at	Mm.133457.1	BB292252		Mm.133457.1	8.43	6.46	7.8	7.69	0.82	4.72	3.95	5.3	4.6	0.53	−1.67	−3.158	.042599
1424978_at	Odf4: outer dense fiber of sperm tails 4	AB074438	252868	Mm.76826.1	25.63	27.97	25.47	26.66	2.03	19.28	17.05	12.3	16.04	2.45	−1.66	−3.338	.03042
1458228_at	Mm.208324.1	BB244358		Mm.208324.1	34.38	30.86	27.78	30.83	2.5	15.11	21.26	20.96	18.76	2.76	−1.64	−3.238	.032194
1453999_at	Urb1: URB1 ribosome biogenesis 1 homolog (S. cerevisiae)	AK017495	207932	Mm.159647.1	93.17	127.33	130.35	117.16	12.34	61.82	64.72	89.94	72.19	9.19	−1.62	−2.922	.047547
1456750_at	B230303O12Rik: RIKEN cDNA B230303O12 gene	BB308463	319739	Mm.131992.1	35.44	40.7	35.94	37.61	2.37	18.67	26.66	24.81	23.21	2.78	−1.62	−3.938	.017838

(continued)

Table 1. Continued

Probe set	Gene	Accession	Entrez Gene	Description	WT-1	WT-2	WT-7	Baseline mean	Baseline mean's SE	MSK-14	MSK-15	MSK-9	Experiment mean	Experiment mean's SE	Fold change	*t* statistic	*p* value
1456166_at	Ehd2: EH-domain containing 2	BB358215	259300	Mm.138215.1	36.02	33.97	38.04	36.04	3.09	25.05	20.96	21.41	22.45	1.79	−1.61	−3.808	.028374
1418552_at	Opn1sw: opsin 1 (cone pigments), short-wave-sensitive (color blindness, tritan)	AF190670	12057	Mm.56987.1	26.24	25.45	22.73	24.79	1.75	12.16	19.88	15.16	15.7	2.56	−1.58	−2.933	.049563
1459451_at	Mm.207852.1	BB201499		Mm.207852.1	29.06	29.62	25.28	27.87	1.63	17.55	14.14	21.39	17.7	2.16	−1.57	−3.754	.022644
1454218_at	4930405D01Rik: RIKEN cDNA 4930405D01 gene	AK015093	73795	Mm.159062.1	25.19	23.46	27.67	25.45	2	15.4	18.17	15.79	16.41	2.03	−1.55	−3.175	.033712
1460064_at	BC028789: cDNA sequence BC028789	BM237812	407802	Mm.103545.1	178.74	142.83	147.97	156	11.67	93.72	107.19	100.39	100.78	5.59	−1.55	−4.266	.025765
1453940_at	2810404M03Rik: RIKEN cDNA 2810404M03 gene	AK012985	69966	Mm.58693.1	25.18	25.89	24.93	25.36	1.09	17.83	14.46	17.64	16.43	1.75	−1.54	−4.339	.018034
1457877_at	Mm.102971.1	AW557111		Mm.102971.1	43.05	35.17	43.94	40.46	3.38	31.21	23.01	23.17	26.28	3.05	−1.54	−3.117	.036131
1440064_at	Etl4: enhancer trap locus 4	BB502547	208618	Mm.169632.1	28.41	34.56	31.93	31.79	2.37	18.69	23.67	19.62	20.77	2.41	−1.53	−3.26	.031089
1445080_at	Mm.218087.1	BG072532		Mm.218087.1	39.92	40.73	41.69	40.69	2.17	19.59	28.99	31.35	26.62	3.93	−1.53	−3.132	.049356
1419932_s_at	Mm.201472.1	AW546472		Mm.201472.1	64.77	57.06	50.76	57.18	4.42	39.07	33	40.49	37.59	2.68	−1.52	−3.791	.02734
1430467_at	4921511H03Rik: RIKEN cDNA 4921511H03 gene	AK014870	70920	Mm.158494.1	77.6	78.23	77.72	77.89	2.68	52.52	52.55	50.77	51.78	2.71	−1.5	−6.861	.002364
1439275_s_at	9530010C24Rik: RIKEN cDNA 9530010C24 gene	BG069453	109279	Mm.11474.1	24.48	26	23.56	24.7	2.21	16.47	16.64	17.1	16.65	1.48	−1.48	−3.032	.04618
1420687_at	4932438H23Rik: RIKEN cDNA 4932438H23 gene	NM_028905	74387	Mm.35184.1	68.09	65.49	61.73	65.01	2.91	40.66	46.74	48.74	45.5	4.04	−1.43	−3.918	.02077
1422273_at	Mmp1b: matrix metallopeptidase 1b (interstitial collagenase)	NM_032007	83996	Mm.156951.1	33.34	28.09	28.03	29.51	2.25	19.57	19.07	23.36	20.63	1.96	−1.43	−2.975	.041925
1426054_at	Npy1r: neuropeptide Y receptor Y1	D63819	18166	Mm.5112.2	39.95	37.39	38.38	38.61	1.93	25.4	28.89	27.29	27.15	3.22	−1.42	−3.051	.049457
1452590_a_at	Gm9780 /// Plac9: predicted gene 9780 /// placenta specific 9	BB609699	100039175 /// 211623	Mm.29491.1	174.21	154.86	173.92	167.36	7.32	138.39	109.58	102.21	117.54	11.88	−1.42	−3.571	.031712
1446429_at	P2rx4: purinergic receptor P2X, ligand-gated ion channel 4	BB110945	18438	Mm.207333.1	48.22	47.42	41.89	45.96	2.16	36.46	30.2	30.82	32.42	2.2	−1.42	−4.398	.011718

(continued)

Table 1. Continued

Probe set	Gene	Accession	Entrez Gene	Description	WT-1	WT-2	WT-7	Baseline mean	Baseline mean's SE	MSK-14	MSK-15	MSK-9	Experiment mean	Experiment mean's SE	Fold change	*t* statistic	*p* value
1418943_at	B230120H23Rik: RIKEN cDNA B230120H23 gene	NM_023057	65964	Mm.33127.1	78.26	87.25	73.14	79.74	4.8	55.89	55.17	57.92	56.44	2.72	−1.41	−4.225	.02179
1432791_at	9030218A15Rik: RIKEN cDNA 9030218A15 gene	AK020251	77662	Mm.159968.1	84.87	86.93	72.67	81.36	4.88	60.11	61.32	50.9	57.74	4.22	−1.41	−3.662	.022334
1445611_at	Trappc9: trafficking protein particle complex 9	BB349535	76510	Mm.179878.1	42.64	53.04	50.98	48.62	3.75	31.68	37.76	33.25	34.39	2.69	−1.41	−3.081	.042056
1443393_at	Mm.131148.1	BB201890		Mm.131148.1	101.79	84.49	83.95	89.71	6.62	60.17	61.83	70.02	64	3.92	−1.4	−3.341	.039369
1446254_at	Mm.149067.1	BB116559		Mm.149067.1	18.33	20.69	19.26	19.53	0.97	12.81	14.52	14.26	13.99	0.91	−1.4	−4.168	.014144
1429358_at	Fam135a: family with sequence similarity 135, member A	AK019549	68187	Mm.87130.1	26.74	24.67	28.35	26.83	1.51	18.14	20.73	18.85	19.34	1.81	−1.39	−3.181	.03506
1457308_at	Mm.4245.1	BG070176		Mm.4245.1	53.25	45.83	43.52	47.65	3.04	32.48	35.7	34.91	34.41	1.41	−1.38	−3.944	.032405
1455000_at	Gpr68: G protein-coupled receptor 68	BB538372	238377	Mm.32160.1	394.3	348.73	339.88	361.88	17.77	264.67	271.46	249.4	262.82	8.79	−1.38	−4.998	.016385
1417017_at	Cyp17a1: cytochrome P450, family 17, subfamily a, polypeptide 1	NM_007809	13074	Mm.1262.1	40.4	38.41	44.27	40.95	2	30.6	30.94	28.96	29.99	1.64	−1.37	−4.234	.014427
1426305_at	Upk1a: uroplakin 1A	AF262335	109637	Mm.25471.1	47.35	47.65	43.06	46.34	2.76	34.58	34.67	32.89	33.85	2.84	−1.37	−3.15	.034557
1429957_at	Krtap26-1: keratin associated protein 26-1	AK009086	69533	Mm.30967.1	55.69	63.18	58.29	58.89	3.59	45.55	45.7	38.18	42.94	3.91	−1.37	−3.003	.040213
1439674_at	Slc4a8: solute carrier family 4 (anion exchanger), member 8	BB436482	59033	Mm.209856.1	169.3	174.08	152.95	166.06	7.22	116.68	139.51	107.92	121.63	10.17	−1.37	−3.562	.027951
1440191_s_at	Leng9: leukocyte receptor cluster (LRC) member 9	AI847494	243813	Mm.45066.1	300.04	285.18	259.66	281.54	12.12	195.64	215.32	206.5	205.28	6.72	−1.37	−5.501	.010637
1420720_at	LOC100044234 /// Nptx2: hypothetical protein LOC100044234 /// neuronal pentraxin 2	NM_016789	100044234 /// 53324	Mm.10099.1	704.37	660.98	662.72	676.22	14.5	471.43	504.6	510.57	495.71	13.63	−1.36	−9.072	.000833
1421414_a_at	Sema6a: sema domain, transmembrane domain (TM), and cytoplasmic domain, (semaphorin) 6A	NM_018744	20358	Mm.9212.1	63.6	64.02	54.08	60.28	3.7	39.32	50.08	44.06	44.31	4.06	−1.36	−2.91	.044143
1459279_at	Mm.126689.1	BB363958		Mm.126689.1	55.94	60.46	51.02	55.53	3.51	37.3	39.75	45.98	40.98	3.28	−1.36	−3.031	.038982

(continued)

Table 1. Continued

Probe set	Gene	Accession	Entrez Gene	Description	WT-1	WT-2	WT-7	Baseline mean	Baseline mean's SE	MSK-14	MSK-15	MSK-9	Experiment mean	Experiment mean's SE	Fold change	*t* statistic	*p* value
1419005_at	Crybb3: crystallin, beta B3	NM_021352	12962	Mm.40616.1	66.16	62.97	62.51	63.63	3.01	49.56	43.73	48.37	47.51	2.99	−1.34	−3.798	.019144
1452243_at	Kcnj14: potassium inwardly rectifying channel, subfamily J, member 14	BB282273	211480	Mm.68170.1	108.27	104.81	94.68	103.54	5.47	85.87	71.34	75.43	77.48	5.03	−1.34	−3.506	.025051
1440757_at	Mm.102276.1	BB750206		Mm.102276.1	42.91	43.21	46.8	44.11	2.3	30.8	32.14	36.29	32.81	2.9	−1.34	−3.057	.040319
1452796_at	Def6: differentially expressed in FDCP 6	AK010356	23853	Mm.60230.1	144.66	149.03	134.86	143.13	5.78	113.52	102.04	105.28	106.87	4.89	−1.34	−4.788	.009322
1459968_at	Mm.170575.1	AW742677		Mm.170575.1	88.81	88.86	80.55	86.07	3.76	60.69	66.9	64.23	64.24	3.83	−1.34	−4.067	.015267
1457860_at	Mm.25024.1	BG066479		Mm.25024.1	39.65	34.63	37.11	37.03	1.7	27.47	28.52	27.54	27.89	1.58	−1.33	−3.944	.017096
1416342_at	Tnc: tenascin C	NM_011607	21923	Mm.980.1	94.53	81.95	87.47	88.46	4.49	67.57	59.55	75.27	67.17	5.19	−1.32	−3.105	.037079
1424934_at	Ugt2b1: UDP glucuronosyltransferase 2 family, polypeptide B1	BC027200	71773	Mm.26741.1	50.01	56.21	49.16	52.09	3.23	40.92	41.66	35.87	39.5	2.58	−1.32	−3.042	.040732
1438755_at	C80068: expressed sequence C80068	BB327213	97810	Mm.188194.1	53.29	53.27	61.41	56.13	3.52	44.21	39.7	44.97	42.51	2.41	−1.32	−3.19	.039515
1448383_at	Mmp14: matrix metallopeptidase 14 (membrane-inserted)	NM_008608	17387	Mm.19945.1	423.82	418.05	360.61	401.33	21.31	321.82	309.99	278.06	303.19	13.85	−1.32	−3.862	.024044
1430755_at	4930452G13Rik: RIKEN cDNA 4930452G13 gene	BF018617	73989	Mm.107775.1	47.47	47.2	47.85	47.57	2.27	37.65	33.2	35.96	36	2.5	−1.32	−3.422	.027121
1442643_at	Kdm6b: KDM1 lysine (K)-specific demethylase 6B	AW912463	216850	Mm.218492.1	103.09	110.15	109.96	107.91	4.65	82.8	87.28	75.59	81.98	5.78	−1.32	−3.497	.02685
1445746_at	Eif4h: Eukaryotic translation initiation factor 4H	BB118894	22384	Mm.208089.1	53.92	57.22	50.99	54.09	3.23	40.76	37.32	45.15	40.93	2.84	−1.32	−3.06	.038463
1441205_at	1700055N04Rik: RIKEN cDNA 1700055N04 gene	AW060340	73458	Mm.54865.1	88.18	86.2	76.36	83.79	4.7	63.09	62.65	66.93	64.12	2.36	−1.31	−3.737	.034366
1460291_at	Cdk6: cyclin-dependent kinase 6	NM_009873	12571	Mm.88747.1	73.38	80.95	68.53	74.06	4.55	60.63	56.01	54.45	57.12	2.66	−1.3	−3.212	.044154
1446273_at	Csmd1: CUB and Sushi multiple domains 1	BB385992	94109	Mm.208954.1	429.51	457.66	393.59	426.78	20.72	332.71	304.42	349.6	329.16	14.79	−1.3	−3.835	.022308
1457346_at	Mm.65379.1	BE649821		Mm.65379.1	7.4	7	8.21	7.54	0.36	6.6	5.79	4.98	5.79	0.47	−1.3	−2.951	.045372
1421393_at		NM_008172	14814	Mm.56936.1	77.42	68.06	76.5	74.53	3.55	61.12	53.64	57.33	57.62	4.43	−1.29	−2.978	.043237

(continued)

Table 1. Continued

Probe set	Gene	Accession	Entrez Gene	Description	WT-1	WT-2	WT-7	Baseline mean	Baseline mean's SE	MSK-14	MSK-15	MSK-9	Experiment mean	Experiment mean's SE	Fold change	*t* statistic	*p* value
	Grin2d: glutamate receptor, ionotropic, NMDA2D (epsilon 4)																
1448786_at	LOC100045163 /// Plbd1: similar to RIKEN cDNA 1100001H23 gene /// phospholipase B domain containing 1	NM_025806	100045163 /// 66857	Mm.3311.1	130.41	135.4	120.8	128.5	6.63	106.39	96.76	96.73	99.94	4.86	−1.29	−3.472	.029347
1429862_at	Pla2g4e: phospholipase A2, group IVE	AV235932	329502	Mm.158770.1	127.91	133.94	141.19	134.48	6.32	103.46	102.9	107.82	104.37	4.34	−1.29	−3.927	.021619
1445205_at	Mm.218112.1	BM122392		Mm.218112.1	118.27	121.04	107.44	115.49	5.69	83.32	86.59	95.75	89.27	4.78	−1.29	−3.53	.025428
1421865_at	Dbil5: diazepam binding inhibitor-like 5	AK006528	13168	Mm.46156.1	96.63	85.01	87.65	89.97	3.82	69.05	69.22	74.34	70.38	2.52	−1.28	−4.287	.017347
1427138_at	Ccdc88c: coiled-coil domain containing 88C	AW556861	68339	Mm.83109.1	228.03	247.07	234.49	236.59	8.43	176.79	185.89	191.17	184.76	7.3	−1.28	−4.646	.010167
1438628_x_at	Cntn3: contactin 3	BB559510	18488	Mm.92049.1	362.31	362.74	351.27	358.71	9.39	262.84	311.68	266.28	279.52	19.44	−1.28	−3.668	.037389
1441477_at	Calu: calumenin	BB120190	12321	Mm.215372.1	69.25	78.1	76.88	74.78	3.88	55.59	56.31	63.08	58.29	4.04	−1.28	−2.945	.042246
1441790_at	Mm.101345.1	AW489900		Mm.101345.1	153.06	149.99	138.28	146.64	5.41	108.19	116.23	121.72	114.81	4.97	−1.28	−4.335	.01249
1447669_s_at	Gng4: guanine nucleotide binding protein (G protein), gamma 4	AV347903	14706	Mm.215394.1	1237.64	1257.84	1328.35	1271.66	33.43	916.3	1000.93	1066.68	995.13	50.1	−1.28	−4.592	.013885
1458793_at	Mm.182870.1	BG076186		Mm.182870.1	62.36	66.12	67.85	65.33	2.66	52.13	51.9	47.56	50.88	2.88	−1.28	−3.687	.02131
1421109_at	Cml2: camello-like 2	NM_053096	93673	Mm.24251.1	239.07	244.64	211.19	232.11	10.96	181.9	185.84	183.29	183.27	4.3	−1.27	−4.149	.033366
1431147_at	Rint1: RAD50 interactor 1	BG807740	72772	Mm.133300.1	150.88	131.25	129.19	136.92	7.24	110.96	111.2	100.08	107.67	4.52	−1.27	−3.425	.035088
1445835_at	Mm.76734.1	AW123001		Mm.76734.1	101.39	90.78	98.14	96.86	3.52	78.84	72.74	78.58	76.31	3.26	−1.27	−4.283	.012982
1426492_at	Tdp1: tyrosyl-DNA phosphodiesterase 1	AK014855	104884	Mm.196233.1	178.5	163.74	167.38	170.45	6.9	134.68	132.37	140.02	135.04	5.34	−1.26	−4.059	.01736
1449537_at	Msh5: mutS homolog 5 (E. coli)	NM_013600	17687	Mm.24192.1	99.27	104.84	114.17	106.25	5.23	74.32	91.75	86.48	84.25	5.76	−1.26	−2.828	.047959
1452035_at	Col4a1: collagen, type IV, alpha 1	BF158638	12826	Mm.738.1	402.93	451.75	470.78	441.6	22.29	326.93	339.27	389.33	350.26	21.58	−1.26	−2.944	.042262
1438203_at	Scarf2: Scavenger receptor class F, member 2	BF467245	224024	Mm.33775.2	39.42	42.7	43.15	41.96	1.98	35.1	30.77	34.85	33.31	1.89	−1.26	−3.152	.034554
1444108_at	Dnajc25: DnaJ (Hsp40) homolog, subfamily C, member 25	AI414004	72429	Mm.211696.1	179.21	171.26	167.4	172.06	4.82	135.68	129.96	144.72	136.88	5.35	−1.26	−4.882	.008377
1444810_at	Mm.182531.1	BG065305		Mm.182531.1	50.56	49.92	48.8	49.67	2.2	37.3	38.74	40.71	39.27	2.29	−1.26	−3.278	.03064
1446975_at		BE949945	69743	Mm.150579.1	144.35	160.17	148.64	150.89	5.83	118.12	130.17	112.08	120.05	6.03	−1.26	−3.679	.021268

(continued)

Table 1. Continued

Probe set	Gene	Accession	Entrez Gene	Description	WT-1	WT-2	WT-7	Baseline mean	Baseline mean's SE	MSK-14	MSK-15	MSK-9	Experiment mean	Experiment mean's SE	Fold change	*t* statistic	*p* value
	Casz1: Castor homolog 1, zinc finger (Drosophila)																
1447433_at	Wdfy3: WD repeat and FYVE domain containing 3	BB743316	72145	Mm.44007.1	321.95	375.48	343.8	347.02	16.18	248.72	279.7	295.72	274.77	14.46	−1.26	−3.329	.029679
1456921_at	Mm.151095.1	BE956991		Mm.151095.1	87.32	87.7	78.92	84.61	3.64	73.68	68.17	59.65	67.41	4.72	−1.26	−2.889	.048063
1421821_at	Ldlr: low density lipoprotein receptor	AF425607	16835	Mm.3213.1	426.43	462.69	401.82	429.93	19.48	357.56	352.59	327.42	345	11.13	−1.25	−3.785	.029189
1426591_at	Gfm2: G elongation factor, mitochondrial 2	BB497484	320806	Mm.219675.1	130.64	135.94	132.44	132.95	4.15	113.34	103.74	104.18	106.77	4.96	−1.25	−4.05	.016453
1450971_at	Gadd45b: growth arrest and DNA-damage-inducible 45 beta	AK010420	17873	Mm.1360.1	509.27	481.26	432.79	473.9	24.02	366.48	369.13	409.23	380.63	16.47	−1.25	−3.203	.039018
1434973_at	Car7: carbonic anhydrase 7	BE650380	12354	Mm.63694.1	327.74	346.25	328.23	333.49	9.26	260.01	283.81	254.63	266.16	10.67	−1.25	−4.767	.009299
1435116_at	4933403G14Rik: RIKEN cDNA 4933403G14 gene	BB219003	74393	Mm.41709.1	176.69	154.36	181	170.68	8.71	130.52	141.79	136.03	136.03	5.72	−1.25	−3.327	.03638
1440834_at	Slc5a10: solute carrier family 5 (sodium/glucose cotransporter), member 10	BB502441	109342	Mm.41011.1	125.08	134.03	115.77	124.55	6.77	98.91	99.31	101.57	99.66	3.46	−1.25	−3.275	.047042
1460478_at	2200002J24Rik: RIKEN cDNA 2200002J24 gene	AK008620	69147	Mm.45301.1	152.68	143.05	136.21	143.49	5.49	108.37	129.08	108.87	115.24	7.8	−1.25	−2.961	.04754
1417170_at	Lztfl1: leucine zipper transcription factor-like 1	NM_033322	93730	Mm.133164.1	432.72	440.32	460.48	444.22	12.58	580.2	528	555.97	554.39	16.92	1.25	5.225	.007956
1417791_a_at	Zfml: zinc finger, matrin-like	BM238431	18139	Mm.4503.1	603.83	584.34	597.44	594.66	13.66	749.91	678.98	797.88	742.26	36.46	1.25	3.791	.042502
1423444_at	Rock1: Rho-associated coiled-coil containing protein kinase 1	BI662863	19877	Mm.6710.1	468.92	526.5	521.12	504.9	20.54	657.71	599.07	631.15	629.09	18.38	1.25	4.506	.011078
1425095_at	BC002059: cDNA sequence BC002059	BC002059	213811	Mm.130624.1	138.71	131.84	140.27	136.08	4.63	174.89	169.53	167.14	170.4	4.4	1.25	5.375	.005832
1425338_at	Plcb4: phospholipase C, beta 4	BB224034	18798	Mm.132097.1	91.63	89.8	97.52	93.36	4.77	123.22	113.3	115.1	116.93	4.46	1.25	3.61	.022714
1427089_at	Ccnt2: cyclin T2	BI872151	72949	Mm.45584.1	268.1	284.73	311.81	289.1	15.34	390.92	349.47	351.96	361.9	15.93	1.25	3.292	.030211

(continued)

Table 1. Continued

Probe set	Gene	Accession	Entrez Gene	Description	WT-1	WT-2	WT-7	Baseline mean	Baseline mean's SE	MSK-14	MSK-15	MSK-9	Experiment mean	Experiment mean's SE	Fold change	*t* statistic	*p* value
1437461_s_at	Rnpc3: RNA-binding region (RNP1, RRM) containing 3	BB557441	67225	Mm.58104.2	131.32	150.69	145.85	142.79	7.28	173.91	164.41	196.42	178.35	9.79	1.25	2.914	.047948
1452659_at	Dek: DEK oncogene (DNA binding)	AK007546	110052	Mm.28343.1	1080.09	1042.17	1035.41	1051.28	19.33	1396.44	1259.97	1280.06	1310.85	44.07	1.25	5.393	.015682
1443857_at	Hook3: hook homolog 3 (Drosophila)	BB825115	320191	Mm.63527.1	195.2	202.63	236.78	211.28	13.35	254.63	257.81	281.53	264.66	9.71	1.25	3.233	.036332
1416421_a_at	Ssb: Sjogren syndrome antigen B	BG796845	20823	Mm.10508.1	378.2	349.83	335.58	354.22	13.47	472.79	403.84	464.8	446.72	22.64	1.26	3.511	.034363
1424410_at	Ttc8: tetratricopeptide repeat domain 8	BC017523	76260	Mm.32328.1	397.32	437.03	429.19	422.1	14.98	565.57	515.61	514.96	532.85	18.4	1.26	4.667	.010504
1424591_at	5830433M19Rik: RIKEN cDNA 5830433M19 gene	BC020067	67770	Mm.35170.1	200.01	179.9	218.2	198.46	11.96	239.31	247.62	263.25	250.4	8.58	1.26	3.528	.028493
1429490_at	Rif1: Rap1 interacting factor 1 homolog (yeast)	AK018316	51869	Mm.27568.1	89.67	86.6	98.15	92.22	4.7	107.72	117.36	123.37	116.35	5.51	1.26	3.329	.030234
1429623_at	Zfp644: zinc finger protein 644	AV261187	52397	Mm.220900.1	525.47	521.94	518.53	521.49	9.12	721.36	625.1	622.19	656.47	32.84	1.26	3.96	.045851
1450994_at	Rock1: Rho-associated coiled-coil containing protein kinase 1	BI662863	19877	Mm.6710.1	370.11	418.42	420.44	404.21	19.67	513.89	485.75	527.24	507.55	15.06	1.26	4.171	.016075
1453162_at	Utp11l: UTP11-like, U3 small nucleolar ribonucleoprotein, (yeast)	AK008801	67205	Mm.156860.2	196.24	213.14	218.74	210.75	10.18	263.21	266.83	263.02	264.69	6.24	1.26	4.517	.016314
1460381_at	Zfp772: zinc finger protein 772	BC023179	232855	Mm.217124.1	95.66	105.05	112.16	104.73	7.4	135.92	127.51	130.19	131.61	3.59	1.26	3.265	.049469
1435348_at	D930009K15Rik: RIKEN cDNA D930009K15 gene	BQ177188	399585	Mm.21093.1	222.36	216.01	229.65	222.37	6.92	291.64	279.52	265.29	279.28	9.07	1.26	4.985	.009008
1435918_at	Fam107a: family with sequence similarity 107, member A	BB277054	268709	Mm.40462.1	471.48	468.07	506.76	482.2	15.99	633.2	638.46	555.75	608.2	28.57	1.26	3.848	.028528
1436116_x_at	Appl1: adaptor protein, phosphotyrosine interaction, PH domain and leucine zipper containing 1	AI585782	72993	Mm.36762.1	209.7	207.81	233	216.29	9.49	259.93	259.84	299.28	273.03	13.62	1.26	3.418	.032037
1455095_at	Hist2h2be: histone cluster 2, H2be	BB667233	319190	Mm.5220.1	209.9	227.54	206.27	214.25	8.88	249.8	285.1	275.44	269.87	12.24	1.26	3.678	.024942
1415855_at	Kitl: kit ligand	BB815530	17311	Mm.4235.1	386.79	459.82	395.51	414.16	25.01	523.41	530.84	516.9	524.2	8.05	1.27	4.189	.037643

(continued)

Table 1. Continued

Probe set	Gene	Accession	Entrez Gene	Description	WT-1	WT-2	WT-7	Baseline mean	Baseline mean's SE	MSK-14	MSK-15	MSK-9	Experiment mean	Experiment mean's SE	Fold change	*t* statistic	*p* value
1424043_at	Ppil4: peptidylprolyl isomerase (cyclo-philin)-like 4	BC004652	67418	Mm.38927.1	499.36	456.12	462.31	473.99	15.39	640.42	580.85	585.05	600.33	20.62	1.27	4.91	.009727
1456319_at	Mm.196322.1	BG065719		Mm.196322.1	72.68	71.1	70.92	71.56	3.43	91.23	98.41	83.27	90.98	5.39	1.27	3.041	.047636
1436446_at	2310007O11Rik: RIKEN cDNA 2310007O11 gene	BQ176469	74177	Mm.37929.1	376.59	401.5	471.85	416.47	29.74	526.38	519.75	546.66	530.29	10.31	1.27	3.615	.049595
1440902_at	Ermn: ermin, ERM-like protein	AI854460	77767	Mm.40963.1	995.28	938.89	788.71	906.19	63.37	1063.38	1252.69	1138.13	1150.5	57.68	1.27	2.851	.046827
1442982_at	Ccdc66: coiled-coil domain containing 66	BG075305	320234	Mm.216841.2	251.06	244.55	253.12	249.23	8.21	327.06	291.38	332.61	316.44	14.24	1.27	4.089	.023368
1455738_at	Ccdc55: coiled-coil domain containing 55	BB066444	237859	Mm.116117.1	143.35	137.24	143.89	141.69	5.19	173.48	193.62	170.54	179.24	9.33	1.27	3.519	.036418
1423445_at	Rock1: Rho-associated coiled-coil containing protein kinase 1	BI662863	19877	Mm.6710.1	309.17	340.28	336.26	328.91	11.68	441.93	397.23	419.64	420.36	14.01	1.28	5.013	.00806
1425575_at	Epha3: Eph receptor A3	M68513	13837	Mm.1977.1	154.74	123.67	130.43	135.57	10.09	166.22	184.06	172.18	174.08	6.61	1.28	3.192	.040815
1452110_at	Mtrr: 5-methyltetrahy-drofolate-homocys-teine methyltransfer-ase reductase	BB757908	210009	Mm.205514.1	230	193.89	239.93	221.39	14.29	303.1	286.52	257.77	282.59	14.11	1.28	3.048	.038106
1456510_x_at	Higd1c /// Mettl7a2: HIG1 domain family, member 1C /// methyltransferase like 7A2	BB703414	380975 /// 393082	Mm.220975.3	254.81	284.04	272.16	269.26	12.51	360.13	345.26	329.26	344.53	11.3	1.28	4.466	.011376
1436139_at	Mm.115096.1	AV328974		Mm.115096.1	143.44	152.61	156.78	151.25	6.56	187.47	186.62	206.57	193.79	7.3	1.28	4.336	.012597
1443986_at	Cdc73: cell division cycle 73, Paf1/RNA poly-merase II complex component, homolog (S. cerevisiae)	BB211070	214498	Mm.123792.1	187.04	152.7	186.86	175.65	11.83	226.38	211.75	235.19	224.69	7.83	1.28	3.458	.032441
1428052_a_at	Zmym1: zinc finger, MYM domain containing 1	BC027750	68310	Mm.80623.2	243.94	257.89	248.99	250.74	7.83	333.63	284.92	348.43	323.04	19.29	1.29	3.473	.048966
1439103_at	Cdc73: cell division cycle 73, Paf1/RNA poly-merase II complex component, homolog (S. cerevisiae)	BB183750	214498	Mm.221175.1	158.8	159.47	161.08	159.69	4.05	204.74	194.33	216.84	205.52	7.05	1.29	5.634	.00934
1449972_s_at		NM_011765	22759 /// 449000	Mm.4596.1	223.44	213.43	207.91	214.67	6.04	273.53	278.11	277.08	276.3	5.89	1.29	7.301	.001877

(continued)

Table 1. Continued

Probe set	Gene	Accession	Entrez Gene	Description	WT-1	WT-2	WT-7	Baseline mean	Baseline mean's SE	MSK-14	MSK-15	MSK-9	Experiment mean	Experiment mean's SE	Fold change	*t* statistic	*p* value
	BC018101 /// Zfp97: cDNA sequence BC018101 /// zinc finger protein 97																
1450954_at	Yme1l1: YME1-like 1 (S. cerevisiae)	BB826168	27377	Mm.23335.1	435.19	451.57	452.69	446.91	11.12	585.37	567.45	582.19	578.33	10.67	1.29	8.528	.001045
1431381_at	3110005L24Rik: RIKEN cDNA 3110005L24 gene	AA611589	73091	Mm.158940.1	70.77	60.44	65.47	65.74	4.37	86.16	81.65	87.44	84.78	3.61	1.29	3.36	.029859
1436157_at	Ccar1: cell division cycle and apoptosis regulator 1	AW538049	67500	Mm.196371.2	926.59	930.69	999.8	952.06	25.61	1267.85	1302.87	1118.49	1228.9	58.62	1.29	4.328	.027373
1447913_x_at	Akap9: A kinase (PRKA) anchor protein (yotiao) 9	BB109183	100986	Mm.131768.1	146.82	157.46	168.26	157.88	7.16	189.82	197.27	223.68	203.53	10.64	1.29	3.559	.029388
1452750_at	5530601H04Rik: RIKEN cDNA 5530601H04 gene	BB820846	71445	Mm.44816.1	205.41	198.8	205.2	203.72	5.39	284.91	264.22	236.06	261.87	15.28	1.29	3.59	.049852
1456027_at	Rbm41: RNA binding motif protein 41	AV315180	237073	Mm.86328.1	127.25	115.89	115.45	119.5	5.25	163.33	154.15	144.21	153.93	6.31	1.29	4.194	.014735
1427518_at	D10627: cDNA sequence D10627	AI892455	234358	Mm.10509.1	103.25	92	92.85	95.42	4.51	125.7	116.81	129.15	123.72	4.84	1.3	4.281	.012974
1439272_at	Lcorl: ligand dependent nuclear receptor corepressor-like	BB183240	209707	Mm.32012.3	188.36	191.61	221.02	200.51	11.72	243.12	247.32	291.93	260.54	16.55	1.3	2.96	.047371
1457897_at	Iqce: IQ motif containing E	AV245518	74239	Mm.23778.1	49.8	51.48	46.73	48.95	2.64	67.09	59.48	62.95	63.4	2.67	1.3	3.847	.01835
1416958_at	Nr1d2: nuclear receptor subfamily 1, group D, member 2	NM_011584	353187	Mm.26587.1	1633.2	1745.68	1893.36	1757.7	79.82	2412.63	2241.99	2271.59	2306.32	56.26	1.31	5.618	.006753
1434150_a_at	Higd1c /// Mettl7a1 /// Mettl7a2: HIG1 domain family, member 1C /// methyltransferase like 7A1 /// methyltransferase like 7A2	AV171622	380975 /// 393082 /// 70152	Mm.220975.2	408.26	453.92	404.75	422.32	18.25	573.73	550.07	527.89	552.11	14.53	1.31	5.564	.005899
1451805_at	Phip: pleckstrin homology domain interacting protein	BI737352	83946	Mm.54737.1	106.83	111.25	103.61	106.99	5.12	145.62	136.2	138.98	139.78	5.31	1.31	4.445	.01132

(continued)

Table 1. Continued

Probe set	Gene	Accession	Entrez Gene	Description	WT-1	WT-2	WT-7	Baseline mean	Baseline mean's SE	MSK-14	MSK-15	MSK-9	Experiment mean	Experiment mean's SE	Fold change	*t* statistic	*p* value
1429690_at	1300003B13Rik: RIKEN cDNA 1300003B13 gene	AK004870	74149	Mm.30767.1	228.26	240.06	231.88	233.59	7.01	314.78	284.94	324.72	307.12	13.19	1.31	4.923	.015498
1436045_at	Tsga10: testis specific 10	AV377349	211484	Mm.40999.1	286	259.77	259.32	267.56	10.91	367.22	347.37	338.68	351.35	12.13	1.31	5.137	.007016
1447854_s_at	Hist2h2be: histone cluster 2, H2be	AV127319	319190	Mm.200193.1	232.85	234.47	231.87	232.95	5	280.32	310.98	325.95	305.48	14.43	1.31	4.749	.027013
1457584_at	AI848100: expressed sequence AI848100	AV377565	226551	Mm.127029.1	34.7	31.13	29.51	31.59	2.43	42.27	38.34	43.49	41.42	2.19	1.31	3.006	.040234
1420340_at	Cspp1: centrosome and spindle pole associated protein 1	NM_026493	211660	Mm.45963.1	119.71	106.74	94.09	106.77	7.66	147.98	143.18	129.63	140.55	5.94	1.32	3.484	.027825
1424672_at	Dmxl1: Dmx-like 1	BC020141	240283	Mm.142349.1	380.03	401.43	455.21	411.76	23.28	531.19	508.47	587.41	542.14	24.05	1.32	3.895	.01765
1429907_at	1700094D03Rik: RIKEN cDNA 1700094D03 gene	AK007060	73545	Mm.3765.1	181.4	137.48	151.82	157.71	13.95	214.27	186.93	222.86	208.59	11.29	1.32	2.834	.04954
1438736_at	Thoc2: THO complex 2	BB703762	331401	Mm.22663.3	462.35	480.2	434.96	458.99	14.62	651.32	562.68	600.5	604.41	26.32	1.32	4.829	.015379
1436540_at	Mirlet7d: microRNA let7d	BQ031149	387247	Mm.26586.1	277.53	305.59	289.56	290.6	10.88	429.91	373.75	349.02	383.83	24.53	1.32	3.475	.045813
1437556_at	Zfhx4: zinc finger homeodomain 4	BF147593	80892	Mm.133521.1	130.93	125.2	162.62	139.33	12.3	185.34	169.98	198.7	184.08	9.22	1.32	2.911	.047873
1438937_x_at	Ang: angiogenin, ribonuclease, RNase A family, 5	AI385586	11727	Mm.202665.1	118.78	104.18	104.62	109.57	6.7	147.4	157.16	128.95	144.74	9.33	1.32	3.062	.042771
1445723_at	Plcl1: phospholipase C-like 1	BB451636	227120	Mm.212111.1	161.24	179.97	157.21	165.82	9.04	219.65	216.86	219.65	219.06	3.15	1.32	5.562	.018683
1436213_a_at	1110028C15Rik: RIKEN cDNA 1110028C15 gene	AV023018	68691	Mm.43671.2	129.89	121.93	141.37	131.16	6.56	170.75	160.26	192.72	174.38	9.89	1.33	3.642	.027896
1434097_at	D10627: cDNA sequence D10627	BM218328	234358	Mm.108679.1	157.36	140.94	141.3	146.46	6.51	186.83	190.43	209.03	195.08	8.05	1.33	4.697	.010337
1424854_at	Hist1h4a /// Hist1h4b /// Hist1h4f /// Hist1h4i /// Hist1h4m: histone cluster 1, H4a /// histone cluster 1, H4b /// histone cluster 1, H4f /// histone cluster 1, H4i /// histone cluster 1, H4m	BC019757	319157 /// 319158 /// 319161 /// 326619 /// 326620	Mm.14775.1	90.2	91.11	74.58	85.87	6.66	126.65	112.52	107.29	115.4	6.44	1.34	3.186	.033408
1451640_a_at	Rsrc2: arginine/serine-rich coiled-coil 2	BC008229	208606	Mm.27799.1	461.19	403.54	438.87	435	17.55	657.47	539.86	546.65	581.73	38.04	1.34	3.502	.043555

(continued)

Table 1. Continued

Probe set	Gene	Accession	Entrez Gene	Description	WT-1	WT-2	WT-7	Baseline mean	Baseline mean's SE	MSK-14	MSK-15	MSK-9	Experiment mean	Experiment mean's SE	Fold change	*t* statistic	*p* value
1433743_at	Dach1: dachshund 1 (Drosophila)	BG075820	13134	Mm.10877.1	66.84	58.07	68.82	64.93	4.03	92.87	78.23	90.29	87.11	4.72	1.34	3.576	.024218
1435230_at	Ankrd12: ankyrin repeat domain 12	BB277613	106585	Mm.34706.1	478.84	465.52	467.21	470.68	9.21	674.29	603.84	613.33	628.85	25.6	1.34	5.814	.016311
1437433_at	B3galt2: UDP-Gal:betaGlcNAc beta 1,3-galactosyltransferase, polypeptide 2	BB254922	26878	Mm.110912.1	179.28	147.72	150.89	159.42	10.59	229.18	201.4	218.88	215.94	8.77	1.35	4.109	.015801
1418526_at	Sfrs13a: splicing factor, arginine/serine-rich 13A	NM_010178	14105	Mm.10229.1	259.28	248.6	283.51	264.54	10.63	388.1	363.75	328.4	359.99	17.79	1.36	4.606	.015941
1418527_a_at	Sfrs13a: splicing factor, arginine/serine-rich 13A	NM_010178	14105	Mm.10229.1	364.64	372.34	392.31	377.18	11.55	568.88	479.73	488.76	512.76	28.77	1.36	4.373	.028901
1449571_at	Trhr: thyrotropin releasing hormone receptor	M59811	22045	Mm.3946.1	238.58	208.05	216.25	221.24	9.75	322.89	261.02	319.94	300.89	20.54	1.36	3.503	.042507
1436156_at	Ccar1: cell division cycle and apoptosis regulator 1	AW538049	67500	Mm.196371.2	523.53	537.22	548.21	537.3	12.02	768.5	751.71	672.18	730.16	30.99	1.36	5.801	.015139
1439340_at	D630036G22Rik: RIKEN cDNA D630036G22 gene	BB501833	442807	Mm.170453.1	38.19	48.15	42.33	42.79	3.57	59.63	62.37	53.04	58.22	3.83	1.36	2.945	.042411
1423084_at	B3galt2: UDP-Gal:betaGlcNAc beta 1,3-galactosyltransferase, polypeptide 2	BB223909	26878	Mm.123510.1	334.31	321.88	340.28	333.24	7.32	463.78	425.19	478.35	455.37	16.85	1.37	6.649	.009263
1448738_at	Calb1: calbindin 1	BB246032	12307	Mm.354.1	170.68	148.33	184.23	167.15	11.55	215.59	234.09	234.64	228.2	8.23	1.37	4.305	.015653
1446261_at	D1Ertd507e: DNA segment, Chr 1, ERATO Doi 507, expressed	BG068111	52356	Mm.155161.1	38.46	36.4	29.53	34.84	3.43	49.18	48.35	46.58	47.9	1.59	1.37	3.454	.04499
1455686_at	Lcorl: ligand dependent nuclear receptor corepressor-like	BB077342	209707	Mm.131615.1	266.79	206.29	270.23	247.61	20.94	332.55	337.08	343.37	338.76	7.44	1.37	4.101	.036974
1458112_at	Adarb2: adenosine deaminase, RNA-specific, B2	BB527550	94191	Mm.190112.1	305.74	288.51	279.66	290.6	10.51	419.59	381.19	394.81	398.53	13.78	1.37	6.229	.004223
1458571_at	D430047D06Rik: RIKEN cDNA D430047D06 gene	BB488016	320716	Mm.135160.1	28.97	25.02	30.16	27.76	2.62	37.76	37.64	38.44	37.93	2.01	1.37	3.076	.040416
1423982_at		AF060490	14105	Mm.10229.2	581.56	587.09	661.64	610.62	26.81	869.42	853.14	830.5	852.39	13.88	1.4	8.009	.004063

(continued)

Table 1. Continued

Probe set	Gene	Accession	Entrez Gene	Description	WT-1	WT-2	WT-7	Baseline mean	Baseline mean's SE	MSK-14	MSK-15	MSK-9	Experiment mean	Experiment mean's SE	Fold change	*t* statistic	*p* value
	Sfrs13a: splicing factor, arginine/serine-rich 13A																
1433322_at	4930529F21Rik: RIKEN cDNA 4930529F21 gene	AK015932	75226	Mm.159470.1	36.51	32.37	29.73	32.88	2.62	50.8	44.24	41.63	46.03	3.39	1.4	3.069	.040568
1447815_x_at	6430527G18Rik: RIKEN cDNA 6430527G18 gene	BB057169	238330	Mm.161505.1	50.64	41.91	39	44.6	4.81	60.44	63.71	64.84	63.05	4	1.41	2.95	.043675
1419014_at	Rhag: Rhesus blood group-associated A glycoprotein	NM_011269	19743	Mm.12961.1	21.82	19.73	18.16	19.94	1.71	31.77	24.51	28.68	28.25	2.31	1.42	2.886	.049339
1456934_at	Calb1: calbindin 1	BB177770	12307	Mm.121403.1	238.21	187.65	224.7	216.7	15.62	337.85	296.9	290.88	308.67	15.52	1.42	4.176	.01396
1430781_at	Ak7: adenylate kinase 7	AV256298	78801	Mm.59172.1	150.21	147.82	138.59	144.92	6.53	228.65	207.74	185.15	207.07	13.38	1.43	4.173	.026715
1437980_at	9130230N09Rik: RIKEN cDNA 9130230N09 gene	BB814947	1E+08	Mm.190421.1	25.6	21.14	26.71	24.54	2.4	35.37	33.64	35.19	35.03	1.96	1.43	3.386	.029338
1439820_at	Mm.167368.1	BB364548		Mm.167368.1	87.31	76.95	69.27	77.64	6.01	123.88	111.09	97.3	111.05	8.06	1.43	3.323	.032963
1457373_at	Mm.135415.1	BB495006		Mm.135415.1	152.34	155.53	181.84	163.77	10.45	251.24	251.9	200.53	234.96	17.83	1.43	3.444	.036695
1443050_at	Fn3krp: fructosamine 3 kinase related protein	BB072270	238024	Mm.117394.1	501.97	591.9	679.4	590.99	52.8	847.83	830.92	870.55	849.75	15.1	1.44	4.712	.031289
1458040_at	D7Wsu130e: DNA segment, Chr 7, Wayne State University 130, expressed	BM213832	28017	Mm.33177.1	47.59	46.86	51.41	49.05	3.07	72.64	74.88	65.4	71.03	3.68	1.45	4.587	.010898
1455087_at	D7Ertd715e: DNA segment, Chr 7, ERATO Doi 715, expressed	AV328498	52480	Mm.21243.1	180.24	158.92	168.84	169.31	6.5	257.55	245.19	236.27	246.39	6.63	1.46	8.302	.001152
1441938_x_at	Cables1: CDK5 and Abl enzyme substrate 1	BB071777	63955	Mm.63141.1	103.77	103.88	145.15	118.01	14.28	166.82	182.08	170.07	173.23	6.02	1.47	3.563	.04495
1450208_a_at	Elmo1: engulfment and cell motility 1, ced-12 homolog (C. elegans)	NM_080288	140580	Mm.214934.1	157.5	179.25	187.87	174.63	10.48	264.19	303.84	222.94	263.69	24.15	1.51	3.383	.049539
1419347_x_at	Svs5: seminal vesicle secretory protein 5	NM_009301	20944	Mm.140154.1	15.98	16.31	12.5	14.93	1.7	25.24	20.45	22.69	22.86	1.69	1.53	3.304	.029812
1448421_s_at	Aspn: asporin	NM_025711	66695	Mm.25755.1	15.78	17.96	14.48	15.96	2.14	22.98	26.37	24.44	24.73	1.88	1.55	3.076	.03789
1417602_at	Per2: period homolog 2 (Drosophila)	AF035830	18627	Mm.8471.1	165.31	180.23	249.94	198.58	26.58	347.55	318.29	266.59	310.75	24.1	1.56	3.126	.035779
1422163_at		NM_008018	14218	Mm.20446.1	9.84	9.73	12.25	11.01	1.45	15.77	18.59	16.62	17.16	1.59	1.56	2.859	.046421

(continued)

Table 1. Continued

Probe set	Gene	Accession	Entrez Gene	Description	WT-1	WT-2	WT-7	Baseline mean	Baseline mean's SE	MSK-14	MSK-15	MSK-9	Experiment mean	Experiment mean's SE	Fold change	*t* statistic	*p* value
	Sh3pxd2a: SH3 and PX domains 2A																
1457534_at	Mm.210151.1	BB481074		Mm.210151.1	30.93	38.4	27.12	32.4	4.79	47.71	55.5	51.01	50.79	3.89	1.57	2.981	.042874
1459281_at	Mm.208534.1	BB182935		Mm.208534.1	4.97	6.95	5.75	5.73	0.89	8.91	9.47	9.21	9.13	0.81	1.59	2.817	.048443
1436330_x_at	Gm7072: predicted gene 7072	BG244780	631624	Mm.25705.1	67.63	68.19	71.69	69.42	3.45	102.57	105.84	126.76	111.61	8.06	1.61	4.813	.02151
1439717_at	Gabrg3: gamma-aminobutyric acid (GABA) A receptor, subunit gamma 3	BB316100	14407	Mm.44821.1	18.62	20.14	29.18	22.49	3.94	36.54	37.03	38.24	37.31	2.89	1.66	3.033	.043228
1437303_at	Il6st: interleukin 6 signal transducer	BI102913	16195	Mm.96748.1	203.93	239.51	305.91	249.74	30.94	374.55	491.68	387.59	418.57	38.63	1.68	3.412	.029031
1430444_at	0610006L08Rik: RIKEN cDNA 0610006L08 gene	AK002255	76253	Mm.81063.1	1	1	1	1	0.16	1.84	1.53	1.84	1.71	0.14	1.71	3.259	.031831
1430376_at	Lrrc9: leucine rich repeat containing 9	AK019545	78257	Mm.160065.1	19.07	20.79	19.38	19.77	1.85	33.09	38	29.83	34.22	3.68	1.73	3.511	.040127
1425618_at	Dhx9: DEAH (Asp-Glu-Ala-His) box polypeptide 9	U91922	13211	Mm.20000.1	5.67	5.61	8.63	6.65	1.15	11.46	11.61	12.71	11.79	0.86	1.77	3.591	.026201
1442809_at	Scn9a: sodium channel, voltage-gated, type IX, alpha	BB452274	20274	Mm.153332.1	16.86	19.48	15.07	17.4	2.12	34.02	34.22	25.01	31.01	3.3	1.78	3.473	.032983
1419962_at	Mm.195371.1	C80871		Mm.195371.1	8.34	8.47	5.99	7.4	1.45	11.81	14.21	14.27	13.39	1.19	1.81	3.19	.035035
1446552_at	Slc12a3: solute carrier family 12, member 3	BB503574	20497	Mm.209611.1	10.86	8.43	12.58	10.54	1.35	14.82	20.23	22.62	19.22	2.35	1.82	3.202	.045117
1420547_at	Galc: galactosylceramidase	BF168119	14420	Mm.5120.1	68.87	69.19	79.15	72.08	7	153.99	147.99	103.53	135.17	16.53	1.88	3.514	.046204
1437824_at	Grid2: glutamate receptor, ionotropic, delta 2	BB334542	14804	Mm.131503.1	6.78	4.29	7.46	6.16	1.39	12.72	10.53	11.66	11.71	1.19	1.9	3.028	.039988
1421317_x_at	Myb: myeloblastosis oncogene	NM_033597	17863	Mm.1202.1	32.94	26.31	21.77	27.11	4.36	57.83	55.9	44.56	52.87	4.67	1.95	4.033	.015838
1449807_x_at	Gabra2: gamma-aminobutyric acid (GABA) A receptor, subunit alpha 2	AV379247	14395	Mm.45112.2	960.49	1094.93	1173.79	1074.31	77.38	1969.95	2148.45	2248.45	2114.56	90.21	1.97	8.753	.001041
1454561_at	9430087B13Rik: RIKEN cDNA 9430087B13 gene	AK020508	77437	Mm.159920.1	7.7	2.5	6.09	5.58	1.64	9.82	12.79	11.87	11.51	1.29	2.06	2.84	.049778
1430218_at		AK016899	67548	Mm.148731.1	7.54	7.78	4.31	6.61	1.8	12	12.79	17.22	14.02	1.89	2.12	2.838	.047103

(continued)

Table 1. Continued

Probe set	Gene	Accession	Entrez Gene	Description	WT-1	WT-2	WT-7	Baseline mean	Baseline mean's SE	MSK-14	MSK-15	MSK-9	Experiment mean	Experiment mean's SE	Fold change	*t* statistic	*p* value
	4933424M12Rik: RIKEN cDNA 4933424M12 gene																
1419321_at	F7: coagulation factor VII	NM_010172	14068	Mm.4827.1	7.75	9.98	12.2	9.72	2.06	25.68	18.56	18.03	20.69	2.67	2.13	3.255	.034136
1453435_a_at	Fmo2: flavin containing monooxygenase 2	AK009753	55990	Mm.34838.1	18.14	18.33	17.86	18.11	2.09	39.95	43.63	33.32	38.96	3.52	2.15	5.095	.011921
1443577_at	Mm.72499.1	AV261494		Mm.72499.1	4.98	5.78	5.82	5.49	0.51	10.74	10.72	14.71	12.04	1.38	2.2	4.468	.029512
1454638_a_at	Pah: phenylalanine hydroxylase	AW106920	18478	Mm.2422.2	1	3.36	2.37	2.27	0.75	4.52	5.68	5.26	5.11	0.58	2.25	2.985	.043983
1420300_at	Mm.45112.2	AV379247		Mm.45112.2	35.8	34.13	30.06	33.09	2.96	69.5	73.24	81.05	74.48	3.97	2.25	8.355	.001566
1420774_a_at	4930583H14Rik: RIKEN cDNA 4930583H14 gene	NM_026358	67749	Mm.62589.1	8.56	4.51	5.51	6.46	2.07	15.78	12.7	17.34	15.41	2.2	2.39	2.963	.04165
1440510_at	C430002N11Rik: RIKEN cDNA C430002N11 gene	BB407702	319707	Mm.140067.1	1	1	1	1	0.24	2.96	2.23	2.23	2.44	0.26	2.44	4.09	.01519
1442860_at	Dgkb: diacylglycerol kinase, beta	BB429621	217480	Mm.208793.1	2.66	5.71	9.12	5.74	2.02	15.91	12.73	14.13	14.18	1.37	2.47	3.467	.031537
1440754_at	Mm.193602.1	BG797192		Mm.193602.1	7.31	3.58	3.32	4.9	1.73	12.89	11.3	12.33	12.3	1.07	2.51	3.633	.030159
1429481_at	Nck2: non-catalytic region of tyrosine kinase adaptor protein 2	AK014772	17974	Mm.144978.1	3.3	6.21	2.6	4.1	1.51	10.66	11.01	9.63	10.45	1.23	2.55	3.258	.032988
1423340_at	Tcfap2b: transcription factor AP-2 beta	AV334599	21419	Mm.4795.1	1	1.87	3.53	2.1	0.9	5.09	6.49	4.95	5.52	0.59	2.63	3.189	.041073
1425434_a_at	Msr1: macrophage scavenger receptor 1	L04274	20288	Mm.1227.2	3.95	1	5.87	3.45	1.56	8.98	7.75	10.51	9.07	1.17	2.63	2.889	.048776
1418783_at	Trpm5: transient receptor potential cation channel, subfamily M, member 5	AF228681	56843	Mm.143747.1	9.47	10.65	3.88	7.72	2.65	21.44	20.09	19.89	20.42	1.38	2.65	4.254	.023746
1453812_at	Jakmip2: janus kinase and microtubule interacting protein 2	AK018295	76217	Mm.165340.1	3.53	6.64	6.07	5.21	2.42	17.24	11.99	13.61	14.22	1.97	2.73	2.895	.046562
1455444_at	Gabra2: gamma-aminobutyric acid (GABA) A receptor, subunit alpha 2	BB339336	14395	Mm.121933.1	691.96	660.47	646.13	666.54	19.81	1812.1	1792.15	1931.73	1843.54	48.15	2.77	22.607	.000409
1451510_s_at		BC025001	99035	Mm.13808.1	1.4	3.4	1.49	2.14	0.76	6.42	6.8	4.87	6.04	0.91	2.82	3.291	.031751

(continued)

Table 1. Continued

Probe set	Gene	Accession	Entrez Gene	Description	WT-1	WT-2	WT-7	Baseline mean	Baseline mean's SE	MSK-14	MSK-15	MSK-9	Experiment mean	Experiment mean's SE	Fold change	*t* statistic	*p* value
	Olah: oleoyl-ACP hydrolase																
1421044_at	Mrc2: mannose receptor, C type 2	BB528408	17534	Mm.9020.1	1	5.57	4.99	3.85	1.52	12.94	8.43	11.37	10.96	1.44	2.85	3.393	.027566
1432837_at	2700080J24Rik: RIKEN cDNA 2700080J24 gene	AK012542	67969	Mm.158180.1	2.82	2.1	5.55	3.43	1.43	9.26	8.57	11.03	9.77	1.06	2.85	3.571	.026743
1421738_at	Gabra2: gamma-aminobutyric acid (GABA) A receptor, subunit alpha 2	NM_008066	14395	Mm.5304.1	586.9	565.56	595.82	582.45	12.02	1703.77	1644.43	1765.13	1705.63	39.55	2.93	27.174	.000522
1459553_at	Mm.172145.1	BG068521		Mm.172145.1	1.75	3.54	1.35	2.01	0.93	5.98	5.42	7.25	6.31	0.83	3.14	3.445	.026706
1451349_at	Efcab7: EF-hand calcium binding domain 7	BC020077	230500	Mm.207859.1	43.05	56.46	59.29	53.06	12.18	177.8	140.15	182.95	166.99	13.96	3.15	6.152	.00376
1430751_at	Serpina3i: serine (or cysteine) peptidase inhibitor, clade A, member 3I	AK019935	628900	Mm.194525.1	2.24	2.06	3.42	2.44	0.87	7.19	7.63	8.76	7.8	0.73	3.2	4.739	.009707
1424233_at	Meox2: mesenchyme homeobox 2	BC002076	17286	Mm.153716.1	1.62	3.86	4.83	3.33	1.82	13.33	8.69	9.68	10.7	1.62	3.21	3.031	.039425
1443865_at	Gabra2: gamma-aminobutyric acid (GABA) A receptor, subunit alpha 2	BQ174589	14395	Mm.45112.1	304.6	268.13	278.64	283.81	11.89	975.16	892.33	949.03	939.04	24.63	3.31	23.956	.000207
1457044_at	Macc1: metastasis associated in colon cancer 1	BB007136	238455	Mm.31376.1	3.07	3.52	3.29	3.31	1.45	11.72	9.59	14.05	11.65	1.88	3.52	3.507	.027354
1450573_at	Amh: anti-Mullerian hormone	NM_007445	11705	Mm.57098.1	3.06	2.53	4.46	3.67	1.6	12.2	10.17	16.74	13.02	1.96	3.54	3.693	.022496
1449393_at	LOC100046930 /// Sh2d1a: similar to T cell signal transduction molecule1 SAP /// SH2 domain protein 1A	NM_011364	100046930 /// 20400	Mm.20880.1	4.55	5.67	1.62	3.59	1.7	18.47	12.96	10.76	14.07	2.31	3.92	3.663	.024942
1419100_at	Serpina3n: serine (or cysteine) peptidase inhibitor, clade A, member 3N	NM_009252	20716	Mm.22650.1	511.9	422.34	563.08	502.61	49.2	2450.79	2136.39	1426.57	2004.13	303.07	3.99	4.89	.03549

(continued)

Table 1. Continued

Probe set	Gene	Accession	Entrez Gene	Description	WT-1	WT-2	WT-7	Baseline mean	Baseline mean's SE	MSK-14	MSK-15	MSK-9	Experiment mean	Experiment mean's SE	Fold change	*t* statistic	*p* value
1419477_at	Clec2d: C-type lectin domain family 2, member d	NM_053109	93694	Mm.197536.1	1.22	1.22	1	1.15	0.27	4.36	4.1	5.66	4.65	0.6	4.06	5.296	.015973
1421564_at	Serpina3c: serine (or cysteine) peptidase inhibitor, clade A, member 3C	NM_008458	16625	Mm.14191.1	10.95	4.35	9.1	8.24	3.68	41.68	32.8	31.41	35.24	3.5	4.28	5.313	.006074
1436170_a_at	Csnl s2a: casein alpha s2-like A	BF119305	12993	Mm.4908.3	1.12	1.5	3.94	2.01	1.34	7.35	8.41	10.81	8.9	1.51	4.43	3.411	.027567
1457274_at	Gm13103: predicted gene 13103	BB555205	194225	Mm.17793.1	1.69	1.22	4.48	2.47	1.22	11.98	9.97	13.96	11.89	1.58	4.81	4.705	.010753

Declaration of Conflicting Interests

The authors declared no potential conflicts of interest with respect to the research, authorship, and/or publication of this article.

Funding

The authors disclosed receipt of the following financial support for the research, authorship, and/or publication of this article: This work was supported by the National Institutes of Health (grant numbers: NS47176, NS066345, and MH062335).

References

Alessandrini, A., Namura, S., Moskowitz, M. A., & Bonventre, J. V. (1999). MEK1 protein kinase inhibition protects against damage resulting from focal cerebral ischemia. *Proc Natl Acad Sci U S A*, *96*, 12866–12869.

Arthur, J. S. (2008). MSK activation and physiological roles. *Front Biosci*, *13*, 5866–5879.

Arthur, J. S., & Cohen, P. (2000). MSK1 is required for CREB phosphorylation in response to mitogens in mouse embryonic stem cells. *FEBS Lett*, *482*, 44–48.

Ballif, B. A., & Blenis, J. (2001). Molecular mechanisms mediating mammalian mitogen-activated protein kinase (MAPK) kinase (MEK)-MAPK cell survival signals. *Cell Growth Differ*, *12*, 397–408.

Baraban, J. M., Fiore, R. S., Sanghera, J. S., Paddon, H. B., & Pelech, S. L. (1993). Identification of p42 mitogen-activated protein kinase as a tyrosine kinase substrate activated by maximal electroconvulsive shock in hippocampus. *J Neurochem*, *60*, 330–336.

Bickler, P. E., Zhan, X., & Fahlman, C. S. (2005). Isoflurane preconditions hippocampal neurons against oxygen-glucose deprivation: Role of intracellular Ca2+ and mitogen-activated protein kinase signaling. *Anesthesiology*, *103*, 532–539.

Borges, K., Gearing, M., McDermott, D. L., Smith, A. B., Almonte, A. G., Wainer, B. H., & Dingledine, R. (2003). Neuronal and glial pathological changes during epileptogenesis in the mouse pilocarpine model. *Exp Neurol*, *182*, 21–34.

Buckmaster, P. S., & Dudek, F. E. (1997). Neuron loss, granule cell axon reorganization, and functional changes in the dentate gyrus of epileptic kainate-treated rats. *J Comp Neurol*, *385*, 385–404.

Cagnol, S., & Chambard, J. C. (2010). ERK and cell death: Mechanisms of ERK-induced cell death—apoptosis, autophagy and senescence. *FEBS J*, *277*, 2–21.

Calabrese, V., Lodi, R., Tonon, C., D'Agata, V., Sapienza, M., Scapagnini, G., Mangiameli, A., Pennisi, G., Stella, A. M., & Butterfield, D. A. (2005). Oxidative stress, mitochondrial dysfunction and cellular stress response in Friedreich's ataxia. *J Neurol Sci*, *233*, 145–162.

Carrier, R. L., Ma, T. C., Obrietan, K., & Hoyt, K. R. (2006). A sensitive and selective assay of neuronal degeneration in cell culture. *J Neurosci Methods*, *154*, 239–244.

Cavazos, J. E., Das, I., & Sutula, T. P. (1994). Neuronal loss induced in limbic pathways by kindling: Evidence for induction of hippocampal sclerosis by repeated brief seizures. *J Neurosci*, *14*, 3106–3121.

Cheng, Y., Cawley, N. X., & Loh, Y. P. (2013). Carboxypeptidase E/NFα1: A new neurotrophic factor against oxidative stress-

induced apoptotic cell death mediated by ERK and PI3-K/AKT pathways. *PLoS One*, *8*, e71578.

Choi, Y. S., Karelina, K., Alzate-Correa, D., Hoyt, K. R., Impey, S., Arthur, J. S., & Obrietan, K. (2012). Mitogen- and stress-activated kinases regulate progenitor cell proliferation and neuron development in the adult dentate gyrus. *J Neurochem*, *123*, 676–688.

Choi, Y. S., Lin, S. L., Lee, B., Kurup, P., Cho, H. Y., Naegele, J. R., Lombroso, P. J., & Obrietan, K. (2007). Status epilepticus-induced somatostatinergic hilar interneuron degeneration is regulated by striatal enriched protein tyrosine phosphatase. *J Neurosci*, *27*, 2999–3009.

Chwang, W. B., Arthur, J. S., Schumacher, A., & Sweatt, J. D. (2007). The nuclear kinase mitogen- and stress-activated protein kinase 1 regulates hippocampal chromatin remodeling in memory formation. *J Neurosci*, *27*, 12732–12742.

Corrêa, S. A., Hunter, C. J., Palygin, O., Wauters, S. C., Martin, K. J., McKenzie, C., McKelvey, K., Morris, R. G., Pankratov, Y., Arthur, J. S., & Frenguelli, B. G. (2012). MSK1 regulates homeostatic and experience-dependent synaptic plasticity. *J Neurosci*, *32*, 13039–13051.

Culmsee, C., & Landshamer, S. (2006). Molecular insights into mechanisms of the cell death program: Role in the progression of neurodegenerative disorders. *Curr Alzheimer Res*, *3*, 269–283.

Curia, G., Longo, D., Biagini, G., Jones, R. S., & Avoli, M. (2008). The pilocarpine model of temporal lobe epilepsy. *J Neurosci Methods*, *172*, 143–157.

Curia, G., Lucchi, C., Vinet, J., Gualtieri, F., Marinelli, C., Torsello, A., Costantino, L., & Biagini, G. (2014). Pathophysiogenesis of mesial temporal lobe epilepsy: Is prevention of damage antiepileptogenic? *Curr Med Chem*, *21*, 663–688.

Deak, M., Clifton, A. D., Lucocq, L. M., & Alessi, D. R. (1998). Mitogen- and stress-activated protein kinase-1 (MSK1) is directly activated by MAPK and SAPK2/p38, and may mediate activation of CREB. *EMBO J*, *17*, 4426–4441.

Duchen, L. W., Eicher, E. M., Jacobs, J. M., Scaravilli, F., & Teixeira, F. (1980). Hereditary leucodystrophy in the mouse: The new mutant twitcher. *Brain*, *103*, 695–710.

Dumka, D., Puri, P., Carayol, N., Lumby, C., Balachandran, H., Schuster, K., Verma, A. K., Terada, L. S., Platanias, L. C., & Parmar, S. (2009). Activation of the p38 Map kinase pathway is essential for the antileukemic effects of dasatinib. *Leuk Lymphoma*, *50*, 2017–2029.

El Mchichi, B., Hadji, A., Vazquez, A., & Leca, G. (2007). p38 MAPK and MSK1 mediate caspase-8 activation in manganese-induced mitochondria-dependent cell death. *Cell Death Differ*, *14*, 1826–1836.

Freund, T. F., Ylinen, A., Miettinen, R., Pitkanen, A., Lahtinen, H., Baimbridge, K. G., & Riekkinen, P. J. (1992). Pattern of neuronal death in the rat hippocampus after status epilepticus. Relationship to calcium binding protein content and ischemic vulnerability. *Brain Res Bull*, *28*, 27–38.

Garrido, Y. C., Sanabria, E. R., Funke, M. G., Cavalheiro, E. A., & Naffah-Mazzacoratti, M. G. (1998). Mitogen-activated protein kinase is increased in the limbic structures of the rat brain during the early stages of status epilepticus. *Brain Res Bull*, *47*, 223–229.

Gass, P., Kiessling, M., & Bading, H. (1993). Regionally selective stimulation of mitogen activated protein (MAP) kinase tyrosine phosphorylation after generalized seizures in the rat brain. *Neurosci Lett*, *162*, 39–42.

Gonzalez-Zulueta, M., Feldman, A. B., Klesse, L. J., Kalb, R. G., Dillman, J. F., Parada, L. F., Dawson, T. M., & Dawson, V. L. (2000). Requirement for nitric oxide activation of p21(ras)/extracellular regulated kinase in neuronal ischemic preconditioning. *Proc Natl Acad Sci U S A*, *97*, 436–441.

Han, B. H., & Holtzman, D. M. (2000). BDNF protects the neonatal brain from hypoxic-ischemic injury in vivo via the ERK pathway. *J Neurosci*, *20*, 5775–5781.

Hauge, C., & Frödin, M. (2006). RSK and MSK in MAP kinase signalling. *J Cell Sci*, *119*, 3021–3030.

Healy, S., Khan, P., He, S., & Davie, J. R. (2012). Histone H3 phosphorylation, immediate-early gene expression, and the nucleosomal response: A historical perspective. *Biochem Cell Biol*, *90*, 39–54.

Hetman, M., Kanning, K., Cavanaugh, J. E., & Xia, Z. (1999). Neuroprotection by brain-derived neurotrophic factor is mediated by extracellular signal-regulated kinase and phosphatidylinositol, 3-kinase. *J Biol Chem*, *274*, 22569–22580.

Hetman, M., & Xia, Z. (2000). Signaling pathways mediating anti-apoptotic action of neurotrophins. *Acta Neurobiol Exp (Wars)*, *60*, 531–545.

Hughes, J. P., Staton, P. C., Wilkinson, M. G., Strijbos, P. J., Skaper, S. D., Arthur, J. S., & Reith, A. D. (2003). Mitogen and stress response kinase-1 (MSK1) mediates excitotoxic induced death of hippocampal neurons. *J Neurochem*, *86*, 25–32.

Jiang, W., Van Cleemput, J., Sheerin, A. H., Ji, S. P., Zhang, Y., Saucier, D. M., Corcoran, M. E., & Zhang, X. (2005). Involvement of extracellular regulated kinase and p38 kinase in hippocampal seizure tolerance. *J Neurosci Res*, *81*, 581–588.

Joo, J. H., & Jetten, A. M. (2010). Molecular mechanisms involved in farnesol-induced apoptosis. *Cancer Lett*, *287*, 123–135.

Kannan-Thulasiraman, P., Katsoulidis, E., Tallman, M. S., Arthur, J. S., & Platanias, L. C. (2006). Activation of the mitogen- and stress-activated kinase 1 by arsenic trioxide. *J Biol Chem*, *281*, 22446–22452.

Karelina, K., Hansen, K. F., Choi, Y. S., DeVries, A. C., Arthur, J. S., & Obrietan, K. (2012). MSK1 regulates environmental enrichment-induced hippocampal plasticity and cognitive enhancement. *Learn Mem*, *19*, 550–560.

Karelina, K., Liu, Y., Alzate-Correa, D., Wheaton, K. L., Hoyt, K. R., Arthur, J. S., & Obrietan, K. (2015). Mitogen and stress-activated kinases 1/2 regulate ischemia-induced hippocampal progenitor cell proliferation and neurogenesis. *Neuroscience*, *285*, 292–302.

Kim, Y. S., Hong, K. S., Seong, Y. S., Park, J. B., Kuroda, S., Kishi, K., Kaibuchi, K, & Takai, Y. (1994). Phosphorylation and activation of mitogen-activated protein kinase by kainic acid-induced seizure in rat hippocampus. *Biochem Biophys Res Commun*, *202*, 1163–1168.

Kuroki, Y., Fukushima, K., Kanda, Y., Mizuno, K., & Watanabe, Y. (2001). Neuroprotection by estrogen via extracellular signal-regulated kinase against quinolinic acid-induced cell death in the rat hippocampus. *Eur J Neurosci*, *13*, 472–476.

Lang, E., Bissinger, R., Fajol, A., Salker, M. S., Singh, Y., Zelenak, C., Ghashghaeinia, M., Gu, S., Jilani, K., Lupescu, A.,

Reyskens, K. M., Ackermann, T. F., Föller, M., Schleicher, E., Sheffield, W. P., Arthur, J. S., Lang, F., & Qadri, S. M. (2015). Accelerated apoptotic death and in vivo turnover of erythrocytes in mice lacking functional mitogen- and stress-activated kinase MSK1/2. *Sci Rep*, *5*, 17316 doi: 10.1038/srep17316.

Lee, B., Butcher, G. Q., Hoyt, K. R., Impey, S., & Obrietan, K. (2005). Activity-dependent neuroprotection and cAMP response element-binding protein (CREB): Kinase coupling, stimulus intensity, and temporal regulation of CREB phosphorylation at serine 133. *J Neurosci*, *25*, 1137–1148.

Lee, B., Cao, R., Choi, Y. S., Cho, H. Y., Rhee, A. D., Hah, C. K., Hoyt, K. R., & Obrietan, K. (2009). The CREB/CRE transcriptional pathway: Protection against oxidative stress-mediated neuronal cell death. *J Neurochem*, *108*, 1251–1265.

Lesuisse, C., & Martin, L. J. (2002). Immature and mature cortical neurons engage different apoptotic mechanisms involving caspase-3 and the mitogen-activated protein kinase pathway. *J Cereb Blood Flow Metab*, *22*, 935–950.

Lopes, M. W., Soares, F. M., de Mello, N., Nunes, J. C., de Cordova, F. M., Walz, R., & Leal, R. B. (2012). Time-dependent modulation of mitogen activated protein kinases and AKT in rat hippocampus and cortex in the pilocarpine model of epilepsy. *Neurochem Res*, *37*, 1868–1878.

Martin, E., Betuing, S., Pagès, C., Cambon, K., Auregan, G., Deglon, N., Roze, E., & Caboche, J. (2011). Mitogen- and stress-activated protein kinase 1-induced neuroprotection in Huntington's disease: Role on chromatin remodeling at the PGC-1-alpha promoter. *Hum Mol Genet*, *20*, 2422–2434.

Martin, P., & Pognonec, P. (2010). ERK and cell death: Cadmium toxicity, sustained ERK activation and cell death. *FEBS J*, *277*, 39–46.

Mattson, M. P. (2003). Excitotoxic and excitoprotective mechanisms: Abundant targets for the prevention and treatment of neurodegenerative disorders. *Neuromolecular Med*, *3*, 65–94.

McCoy, C. E., Campbell, D. G., Deak, M., Bloomberg, G. B., & Arthur, J. S. (2005). MSK1 activity is controlled by multiple phosphorylation sites. *Biochem J*, *387*, 507–517.

Moens, U., & Kostenko, S. (2013). Structure and function of MK5/PRAK: The loner among the mitogen-activated protein kinase-activated protein kinases. *Biol Chem*, *394*, 1115–1132.

Mori, M., Burgess, D. L., Gefrides, L. A., Foreman, P. J., Opferman, J. T., Korsmeyer, S. J., Cavalheiro, E. A., Naffah-Mazzacoratti, M. G., & Noebels, J. L. (2004). Expression of apoptosis inhibitor protein Mcl1 linked to neuroprotection in CNS neurons. *Cell Death Differ*, *11*, 1223–1233.

Mu, M. M., Koide, N., Hassan, F., Islam, S., Sugiyama, T., Ito, H., Mori, I., Yoshida, T., & Yokochi, T. (2005). A role of mitogen and stress-activated protein kinase 1/2 in survival of lipopolysaccharide-stimulated RAW 264.7 macrophages. *FEMS Immunol Med Microbiol*, *43*, 277–286.

Nguyen, T. V., Yao, M., & Pike, C. J. (2005). Androgens activate mitogen-activated protein kinase signaling: Role in neuroprotection. *J Neurochem*, *94*, 1639–1651.

Odgerel, T., Kikuchi, J., Wada, T., Shimizu, R., Kano, Y., & Furukawa, Y. (2010). MSK1 activation in acute myeloid leukemia cells with FLT3 mutations. *Leukemia*, *24*, 1087–1090.

Olney, J. W., de Gubareff, T., & Labruyere, J. (1983). Seizure-related brain damage induced by cholinergic agents. *Nature*, *301*, 520–522.

Park, E. M, Joh, T. H., Volpe, B. T., Chu, C. K., Song, G., & Cho, S. (2004). A neuroprotective role of extracellular signal-regulated kinase in N-acetyl-O-methyldopamine-treated hippocampal neurons after exposure to in vitro and in vivo ischemia. *Neuroscience*, *123*, 147–154.

Pedersen, W. A., Wan, R., Zhang, P., & Mattson, M. P. (2002). Urocortin, but not urocortin II, protects cultured hippocampal neurons from oxidative and excitotoxic cell death via corticotropin-releasing hormone receptor type I. *J Neurosci*, *22*, 404–412.

Portt, L., Norman, G., Clapp, C., Greenwood, M., & Greenwood, M. T. (2011). Anti-apoptosis and cell survival: A review. *Biochim Biophys Acta*, *1813*, 238–259.

Racine, R. J. (1972). Modification of seizure activity by electrical stimulation. II. Motor seizure. *Electroencephalogr Clin Neurophysiol*, *32*, 281–294.

Reyskens, K. M., & Arthur, J. S. (2016). Emerging roles of the mitogen and stress activated kinases MSK1 and MSK2. *Front Cell Dev Biol*, *4*, 56.

Rueda, C. B., Llorente-Folch, I., Traba, J., Amigo, I., Gonzalez-Sanchez, P., Contreras, L., Juaristi, I., Martinez-Valero, P., Pardo, B., Del Arco, A., & Satrustegui, J. (2016). Glutamate excitotoxicity and Ca2+-regulation of respiration: Role of the Ca2+ activated mitochondrial transporters (CaMCs). *Biochim Biophys Acta*, *1857*, 1158–1166.

Sakamoto, K., Karelina, K., & Obrietan, K. (2011). CREB: A multifaceted regulator of neuronal plasticity and protection. *J Neurochem*, *116*, 1–9.

She, Q. B., Ma, W. Y., Zhong, S., & Dong, Z. (2002). Activation of JNK1, RSK2, and MSK1 is involved in serine 112 phosphorylation of Bad by ultraviolet B radiation. *J Biol Chem*, *277*, 24039–24048.

Soloaga, A., Thomson, S., Wiggin, G. R., Rampersaud, N., Dyson, M. H., Hazzalin, C. A., Mahadevan, L. C., & Arthur, J. S. (2003). MSK2 and MSK1 mediate the mitogen- and stress-induced phosphorylation of histone H3 and HMG-14. *EMBO J*, *22*, 2788–2797.

Subramaniam, S., & Unsicker, K. (2010). ERK and cell death: ERK1/2 in neuronal death. *FEBS J*, *277*, 22–29.

Sun, C., Mtchedlishvili, Z., Bertram, E. H., Erisir, A., & Kapur, J. (2007). Selective loss of dentate hilar interneurons contributes to reduced synaptic inhibition of granule cells in an electrical stimulation-based animal model of temporal lobe epilepsy. *J Comp Neurol*, *500*, 876–893.

Tang, F. R., & Loke, W. K. (2010). Cyto-, axo- and dendro-architectonic changes of neurons in the limbic system in the mouse pilocarpine model of temporal lobe epilepsy. *Epilepsy Res*, *89*, 43–51.

Tominaga, K., Matsuda, J., Kido, M., Naito, E., Yokota, I., Toida, K., Ishimura, K., Suzuki, K., & Kuroda, Y. (2004). Genetic background markedly influences vulnerability of the hippocampal neuronal organization in the ''twitcher'' mouse model of globoid cell leukodystrophy. *J Neurosci Res*, *77*, 507–516.

Vermeulen, L., Vanden Berghe, W., Beck, I. M., De Bosscher, K., & Haegeman, G. (2009). The versatile role of MSKs in transcriptional regulation. *Trends Biochem Sci*, *34*, 311–318.

Wenger, D. A., Rafi, M. A., Luzi, P., Datto, J., & Costantino-Ceccarini, E. (2000). Krabbe disease: Genetic aspects and progress toward therapy. *Mol Genet Metab*, *70*, 1–9.

White, H. S. (2002). Animal models of epileptogenesis. *Neurology*, *59*, S7–S14.

Wiggin, G. R., Soloaga, A., Foster, J. M., Murray-Tait, V., Cohen, P., & Arthur, J. S. (2002). MSK1 and MSK2 are required for the mitogen- and stress-induced phosphorylation of CREB and ATF1 in fibroblasts. *Mol Cell Biol*, *22*, 2871–2881.

Zhang, S., Khanna, S., & Tang, F. R. (2009). Patterns of hippocampal neuronal loss and axon reorganization of the dentate gyrus in the mouse pilocarpine model of temporal lobe epilepsy. *J Neurosci Res*, *87*, 1135–1149.

Zhuang, S., & Schnellman, R. G. (2006). A death-promoting role for extracellular signal-regulated kinase. *J Pharmacol Exp Ther*, *319*, 991–997.